Cumulative effects of weak pressure waves during the induction period of a thermal explosion in a closed cylinder

By R. KLEIN AND N. PETERS

Institut für Allgemeine Mechanik, RWTH Aachen, West Germany

It is shown that the accumulation of small-amplitude gasdynamic perturbations is able to accelerate the process of self-ignition of a homogeneous explosive mixture. For analytical simplicity, the chemical kinetics are represented by a one-step irreversible reaction with a large activation energy. A one-dimensional piston–cylinder geometry is considered, which allows a slow compression of the gas during the induction period. It is assumed that the rates of temperature increase due to the reaction and due to the compression are comparable. A two-timescale asymptotic expansion for small Mach numbers is performed considering the distinguished limit $ME = O(1)$, where E is the non-dimensional activation energy, and M is the Mach number based on a characteristic speed of the gas motion. Gasdynamic–chemical interaction is observed at the second order, where the secular equations describing the evolution on the slow timescale explicitly show a cumulative influence.

1. Introduction

In many practical combustion systems the Mach number, typically based on the flame speed, is very small. In the limit of zero Mach number the pressure is spatially uniform, which leads to considerable simplification in the analysis. Such a treatment, however, ignores the fact that combustion chemistry is very sensitive to temperature perturbations. Owing to this sensitivity even weak pressure waves may cause temperature perturbations that are large enough to change the reaction rates by an $O(1)$ amount.

Clarke (1978) has considered the interaction of small-amplitude gasdynamic disturbances (including weak shock waves) with a large-activation-energy reaction. He found important effects in a regime where the amplitudes of the disturbances are of the same order of magnitude as the inverse of the non-dimensional activation energy. Since his analysis is restricted to simple waves in an unconfined atmosphere, he can follow the evolution of the wave amplitude along a characteristic line. One important result is that the time to ignition is significantly reduced by an initial compression, such that a local explosion occurs first on the characteristic that has the largest initial pressure disturbance.

Clarke & Cant (1984) investigated a model for the shock-tube autoignition experiment. In this model a strong shock is generated by the impulsive start of a piston. The shock initiates the induction process that usually precedes autoignition in a premixed explosive gas. It is shown that the time to ignition lies between the values calculated for constant-density and for constant-pressure conditions. Driven

by thermal expansions due to the onset of chemical reactions, an acoustic flow field evolves between the piston and the shock. Two characteristic coordinates are introduced to account for wavelets that travel in opposite directions. It is shown how the state of any fluid particle in the field is influenced by acoustic perturbations arriving on wavepaths, as well as by the chemical reaction that has taken place in the fluid particle itself. Up to ignition, deviations from the initial state behind the shock are small such that the dependent variables are expanded around their constant initial values.

On the other hand, G. H. Schneider (1979) considered leading-order variations of the dependent variables in his study of the slow compression of an inert gas in a one-dimensional piston–cylinder system. His objective was to show how the accumulation of multiple reflected weak shock waves leads to a bulk pressure rise corresponding to quasi-static and adiabatic compression. To account for the slow $O(1)$-changes of the dependent variables Schneider used multiple scaling based on the short acoustic time and the long timescale of the piston motion. A characteristic formulation was employed in order to calculate the paths of the weak shocks in terms of Lagrangian coordinates, but no uniformly valid solution for the coordinate perturbations was derived (cf. also W. Schneider 1978).

Recently, Radwhan & Kassoy (1984) investigated the behaviour of a confined inert gas, which is subject to moderate heating at the boundary. An acoustic time analysis shows how gas expansions in the initially thin conduction layers cause acoustic perturbations in the isentropic core of the system. After long times of heating the conduction-dominated regions are no longer small, and by means of a multiple timescaling the evolution of the acoustic flow field on a slowly varying mean field is described. It is argued that the acoustic disturbances are too weak to steepen up to shock waves, and thus there is no need to perform a characteristic transformation.

One of the easiest examples where chemistry is important is thermal self-ignition. Recently, there has been a renewed interest in thermal ignition theory in relation to the problem of engine knock. In a reciprocating engine, combustion takes place in a highly turbulent flow field whose properties are not well understood. Although several gasdynamic and chemical mechanisms have been proposed in the past to explain engine knock, it is not possible to decide which one dominates under the various operating conditions of an engine. A classical explanation is the autoignition of the unburnt gas before the arrival of the flame. If the end gas could be assumed to be entirely homogeneous, thermal runaway would depend on the chemistry alone. However, since acoustic waves traverse the end gas, we believe that chemical–acoustic interactions must also be considered.

2. Formulation

We assume that, in the combustion chamber of a spark-ignition engine, weak pressure waves are generated by fast variations of heat release within the turbulent flame, including localized explosions. These waves traverse the zone of the unburnt end gas and are reflected repeatedly at the boundaries. We expect a cumulative influence of the pressure waves on the evolution of the chemical reactions in the unburnt gas. In addition, the end gas undergoes a slow bulk compression due to the thermal expansion of the burning gas in the flame. We shall refer to this effect as thermal compression in the following. It is expected that, for a certain range of pressure wave amplitudes and a sufficiently high temperature sensitivity of the

reaction rates, there is an acceleration of the autoignition process due to the background compression as well as due to direct interactions of the pressure waves with the chemical reaction. We shall now explain the model problem and define a distinguished asymptotic limit by introducing characteristic timescales for the several processes involved and by specifying their relative orders of magnitude.

The chemical ignition process is characterized by the ignition delay time t_I, which is the time span of the induction process preceding autoignition in a homogeneous system at constant density. This definition will be used throughout, whereas for the time interval of thermal runaway in the non-homogeneous systems, to be considered below, we shall employ the term 'time to ignition'. The ignition delay time t_I only depends on the kinetic properties of the reaction process and on the initial pressure and temperature. In the present work the chemistry will be modelled by an exothermic first-order irreversible reaction with an Arrhenius-type temperature dependence of the reaction rate r, given by

$$r = BY \exp\left(-\frac{E}{RT}\right), \tag{2.1}$$

where Y is the fuel mass fraction, T the temperature, R the specific gas constant, B the frequency factor and E the activation energy. If the non-dimensional activation energy E/RT_a is large, Frank–Kamenetskii's classical theory of thermal runaway shows that the ignition delay time is given by

$$t_I = \frac{\epsilon \exp(1/\epsilon)}{BY_a \gamma(-\Delta h)/c_p T_a}, \quad \epsilon = \frac{RT_a}{E} \ll 1. \tag{2.2}$$

Here $-\Delta h$ is the heat of reaction; $\gamma = c_p/c_v$, where c_p and c_v are the specific heat capacities at constant pressure and volume, respectively, and it is assumed that $c_p = \gamma R/(\gamma-1)$ is constant. The subscript a denotes initial averaged quantities. During the induction stage of the ignition process the rate of temperature increase is $O(\epsilon)$, when measured in units of T_a/t_I. This suggests the definition of the characteristic reaction timescale

$$t_r = \frac{t_I}{\epsilon}, \tag{2.3}$$

which is not an independent scale in the asymptotic regime but will prove to be useful in later discussions. Another important time, provided by the speed of pressure wave propagation, is

$$t_s = \frac{l}{a_a}. \tag{2.4}$$

Here a_a is the initial average speed of sound and l is a characteristic length of the system. The pressure waves induce a characteristic gas velocity u_g, thereby giving rise to the definition of

$$t_g = \frac{l}{u_g}, \tag{2.5}$$

the characteristic time of the gas motion. If, in addition, there is an overall thermal compression an additional timescale appears,

$$t_p = \left(\frac{1}{\rho}\frac{d\rho}{dt}\right)_a^{-1}, \tag{2.6}$$
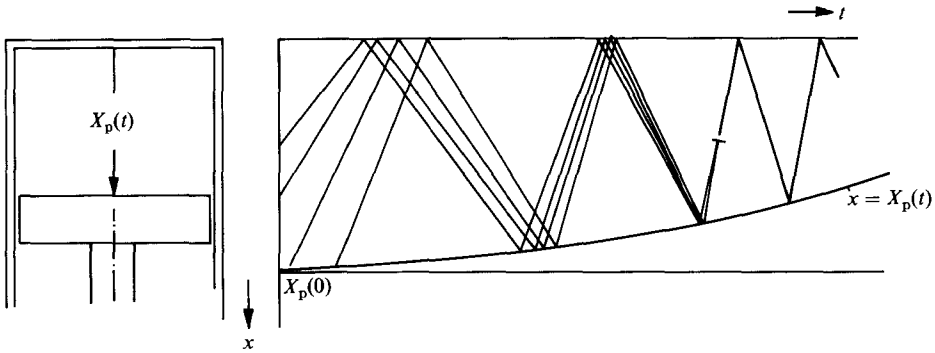
FIGURE 1. The model: a reactive gas compressed within a piston–cylinder system undergoing
additional pressure perturbations.

which characterizes the rate of compression. It is important to keep in mind, that
there is no direct physical connection between the pressure waves and the rate of
thermal compression of the end gas. Therefore t_g and t_p may be chosen independently.

In summary, the problem is to be formulated such that the simultaneous influence
of thermal compression and of many acoustic perturbations on the thermal runaway
of an explosive gas in a combustion chamber can be investigated. Both these effects
will be simulated by a closed piston–cylinder system, in which a slow piston motion
causes a bulk compression and in which appropriate initial conditions create the
desired pressure waves (cf. figure 1). For this model the timescales t_g and t_p can be
expressed as $t_g = X_p(0)/u_g$ and $t_p = X_p(0)/\max(U_p)$, where u_g is a gas velocity
characterizing the initial perturbations and $U_p = dX_p/dt$ is the prescribed piston
velocity.

Although we assume small-amplitude disturbances, we are faced with the
nonlinearities of gasdynamic wave propagation. These will become important due to
accumulation over many acoustic time periods. Following the work of G. H.
Schneider (1979) we employ the analytical method of characteristics together with
the method of multiple timescaling in order to obtain an accurate description of the
wave propagation valid even for long periods of time. (Reviews of these perturbation
methods can be found in Kluwick 1981 and W. Schneider 1978.)

In §3 we first consider a chemically inert gas at constant entropy and develop the
principle steps of the method. As a small expansion parameter the Mach number

$$M = \frac{t_s}{t_g} \ll 1 \tag{2.7}$$

will be used. For the special case that the gasdynamic disturbances are assumed to
result from the piston motion, such that

$$\frac{t_p}{t_g} = O(1), \tag{2.8}$$

our leading-order solution coincides with G. H. Schneider's result revealing the
quasi-static compression as an asymptotic limit. In addition, a nonlinear equation
for the slow time evolution of the pressure perturbations is derived, which describes
the steepening of initially smooth waves up to weak shocks.

In §4 we investigate the thermal runaway. First, in §4.1, we neglect the gas-

dynamic disturbances and consider the case of homogeneous compression. It turns out that rather weak rates of compression acting on the timescale t_r are sufficient to cause an $O(1)$-change of the time to ignition. Thus, wherever a chemically active gas is considered in the following, we restrict the characteristic time t_p of the piston motion to obey

$$\frac{t_p}{t_r} = O(1).$$ (2.9)

In §4.2 we approach the complete model problem of the ignition of a slowly compressed reactive gas, which is perturbed by multiple reflected weak pressure waves. A simple consideration of the reaction rate r shows that a considerable influence of the pressure waves on the chemical reaction appears, if the Mach number, measuring the amplitudes of pressure and temperature, and the activation-energy parameter ϵ, describing the temperature sensitivity of the chemical reactions, are of the same order of magnitude. Thus we consider the distinguished limit

$$\frac{M}{\epsilon} = O(1), \quad \epsilon \to 0.$$ (2.10)

Since we are interested in a cumulative interaction we now set

$$M = \frac{t_s}{t_I} \ll 1$$ (2.11)

such that the pressure waves pass the cylinder many times before ignition takes place. Employing this new definition of M we can use the ratio t_g/t_I to measure the initial amplitudes of the disturbances. The appropriate scaling is

$$\frac{t_g}{t_I} = O(1).$$ (2.12)

Also, with (2.3), and (2.9) and (2.10) it follows that

$$\frac{t_p}{t_I} = O\left(\frac{1}{\epsilon}\right) = O\left(\frac{1}{M}\right).$$ (2.13)

Note that in the ignition problem the perturbations can no longer result from the same mechanism as the bulk compression, since the piston and gas velocities differ by an order of magnitude.

The relevance of the regime stated in (2.11)–(2.13) can be supported by considering the typical pressure–crank angle diagram given in figure 2. The characteristic time t_s of wave propagation is estimated to be

$$t_s = \frac{l}{a_a} \approx 1.7 \times 10^{-5} \text{ s,}$$

where $l \approx 10^{-2}$ m is a characteristic height of the combustion chamber and $a_a \approx 590$ m/s is the speed of sound in air at $p = 60$ bar, calculated under the assumption of an isentropic compression starting from ambient conditions with $T_0 = 273$ K, $p_0 = 1$ atm. During the gas exchange one observes velocities of about 30 m/s, such that

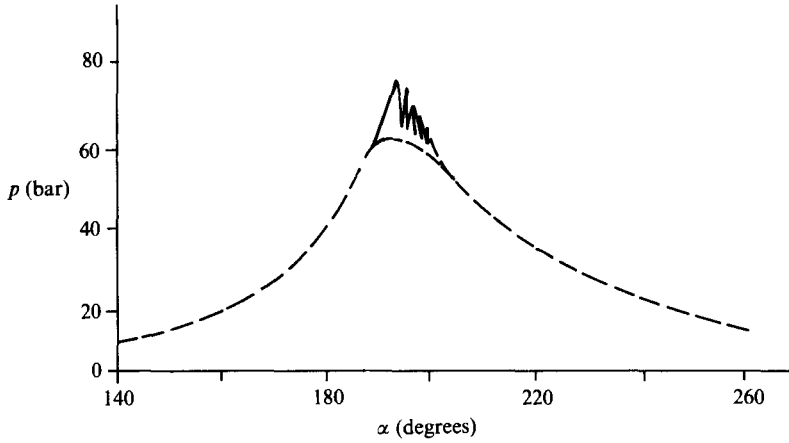$$t_g = \frac{l}{u_g} \approx 3 \times 10^{-4} \text{ s.}$$

FIGURE 2. A typical pressure–crank angle diagram of a knocking engine.

Assuming that the thermal compression of the end gas is nearly isentropic, one may estimate t_p in terms of the slope $dp/d\alpha$ of the pressure with respect to the crank angle in the vicinity of the point of knock by

$$t_p = \left(\frac{1}{\gamma p_{max}}\frac{dp}{d\alpha}2\pi n\right)^{-1} \approx 6 \times 10^{-3}\ \text{s},$$

where we have assumed $n = 2500$ r.p.m. for the engine speed and read $dp/d\alpha$ as one bar per degree crank angle from the diagram. We finally obtain

$$\frac{t_g}{t_s} \approx 18, \quad \frac{t_p}{t_s} \approx 350,$$

which justifies the scalings $t_g/t_s = O(1/M)$ and $t_p/t_s = O(1/M^2)$ suggested by (2.11)–(2.13).

2.1. *Governing equations*

The balance equations for mass, momentum, energy and fuel mass fraction, written in Eulerian coordinates (x, t), and the equation of state, are

$$\left.\begin{aligned}
&\frac{\partial \rho}{\partial t} + \frac{\partial(\rho u)}{\partial x} = 0, \\[6pt]
&\rho\left(\frac{\partial u}{\partial t} + u\frac{\partial u}{\partial x}\right) = -\frac{\partial p}{\partial x}, \\[6pt]
&\rho c_p\left(\frac{\partial T}{\partial t} + u\frac{\partial T}{\partial x}\right) - \left(\frac{\partial p}{\partial t} + u\frac{\partial p}{\partial x}\right) = (-\Delta h)\rho r, \\[6pt]
&\frac{\partial Y}{\partial t} + u\frac{\partial Y}{\partial x} = -r, \\[6pt]
&p = \rho R T,
\end{aligned}\right\} \qquad (2.14)$$

where we have employed the usual symbols ρ, p, T, u for density, pressure temperature and velocity respectively.

Boundary conditions are prescribed for the velocity by

$$u(0,t) = 0, \quad u(X_p(t), t) = \frac{\mathrm{d}X_p(t)}{\mathrm{d}t} \equiv U_p(t), \tag{2.15}$$

while the initial conditions will be given later.

We introduce non-dimensional quantities, dividing p, ρ, T, Y and $a = (\gamma p / \rho)^{\frac{1}{2}}$ by their initial averages p_a, ρ_a, T_a, Y_a, a_a. The reference time t_a will be taken to be equal to t_g in §3 and equal to t_I in §4. In addition we introduce the non-dimensional quantities

$$x^* = \frac{x}{X_p(0)}, \quad u^* = \frac{1}{M}\frac{u}{a_a}, \quad M = \frac{X_p(0)}{a_a t_a}, \tag{2.16a,b,c}$$

$$(-\Delta h)^* = \frac{(-\Delta h) Y_a}{c_p T_a}, \quad \frac{\gamma}{\gamma - 1} = \frac{c_p}{R}, \tag{2.16d,e}$$

$$r^* = \frac{1}{\epsilon} t_a r, \quad t_I^* = \frac{t_I}{t_a}. \tag{2.16f,g}$$

When the non-dimensional reaction rate r^* is of $O(1)$ the regime of (2.3) is obtained, as will be seen in §4.1. In the following we shall suppress the asterisk for non-dimensional quantities but will indicate dimensional quantities by a prime.

Since the total mass in the system is constant, it is convenient to replace x by the Lagrangian coordinate

$$\psi = \frac{\displaystyle\int_0^x \rho(s,t)\,\mathrm{d}s}{\displaystyle\int_0^{X_p(t)} \rho(s,t)\,\mathrm{d}s}. \tag{2.17}$$

The non-dimensional equations are then

$$\frac{\partial \rho}{\partial t} + \rho^2 \frac{\partial u}{\partial \psi} = 0, \tag{2.18a}$$

$$M^2 \gamma \frac{\partial u}{\partial t} + \frac{\partial p}{\partial \psi} = 0, \tag{2.18b}$$

$$\rho \frac{\partial T}{\partial t} - \frac{\gamma - 1}{\gamma} \frac{\partial p}{\partial t} = \epsilon \rho (-\Delta h) r = \epsilon \frac{1}{\gamma t_I} \rho Y \exp\left(\frac{1}{\epsilon}\left(1 - \frac{1}{T}\right)\right), \tag{2.18c}$$

$$\frac{\partial Y}{\partial t} = -\epsilon r, \tag{2.18d}$$

$$p = \rho T. \tag{2.18e}$$

The boundary conditions become

$$u(0,t) = 0, \quad u(1,t) = U_p(t). \tag{2.19}$$

For the later analysis it is convenient to introduce a modified pressure function P and an entropy function S by

$$P = p^{\frac{\gamma - 1}{2\gamma}}, \quad S^2 P^2 = T. \tag{2.20a,b}$$

Then the energy equation simplifies to

$$2P^2 S \frac{\partial S}{\partial t} = \epsilon(-\Delta h) r, \tag{2.21}$$

and the initial conditions are prescribed in terms of u, P, S, Y as

$$
\left.
\begin{aligned}
u(\psi, 0) &= u_{\mathrm{i}}(\psi), \\
P(\psi, 0) &= 1 + \frac{\gamma - 1}{2} M P_{\mathrm{i}}(\psi), \\
S(\psi, 0) &= Y(\psi, 0) = 1,
\end{aligned}
\right\}
\tag{2.22}
$$

where u_{i} and P_{i} are quantities of order unity.

2.2. *Characteristic formulation*

In order to obtain a satisfactory resolution of the wave propagation we first introduce a fast-time coordinate

$$
\tau = \frac{1}{M} t
\tag{2.23}
$$

into (2.18) and perform a transformation to characteristic coordinates (ξ, η) (cf. Appendix A for the derivation).

Lines of constant ξ and η, representing the paths of acoustic waves in the Lagrangian space, are defined by

$$
\frac{\partial \psi}{\partial \xi} - \frac{P^{\Gamma}}{S} \frac{\partial \tau}{\partial \xi} = 0, \quad \frac{\partial \psi}{\partial \eta} + \frac{P^{\Gamma}}{S} \frac{\partial \tau}{\partial \eta} = 0
\tag{2.24}
$$

respectively, where $\Gamma = (\gamma + 1)/(\gamma - 1)$.

When we account for chemical reactions, the particle paths

$$
\psi = \mathrm{const.}
\tag{2.25}
$$

form a third set of characteristics. Along the characteristic curves, changes of the dependent variables must obey the compatibility relations

$$
\frac{\partial P}{\partial \xi} + M \frac{\gamma - 1}{2} \frac{1}{S} \frac{\partial u}{\partial \xi} = \epsilon M \frac{\gamma - 1}{2} \frac{(-\Delta h)}{P S^2} \frac{r}{} \frac{\partial \tau}{\partial \xi},
\tag{2.26a}
$$

$$
\frac{\partial P}{\partial \eta} - M \frac{\gamma - 1}{2} \frac{1}{S} \frac{\partial u}{\partial \eta} = \epsilon M \frac{\gamma - 1}{2} \frac{(-\Delta h)}{P S^2} \frac{r}{} \frac{\partial \tau}{\partial \eta},
\tag{2.26b}
$$

$$
\frac{\partial S}{\partial \tau} = \tfrac{1}{2} M \epsilon (-\Delta h) \frac{r}{S P^2},
\tag{2.26c}
$$

$$
\frac{\partial Y}{\partial \tau} = -M \epsilon r.
\tag{2.26d}
$$

To complete the formulation of the problem, boundary and initial conditions have to be expressed in terms of characteristic coordinates. Since the boundary conditions are imposed on $\psi = 0$, $\psi = 1$ and $\tau = 0$, while (2.24)–(2.26) are written in terms of ξ, η and τ, we have to introduce additional unknown functions

$$
\eta_{\mathrm{c}}(\xi), \quad \xi_{\mathrm{p}}(\eta), \quad \xi_{\mathrm{i}}(\eta)
\tag{2.27}
$$

which represent the top of the cylinder, the piston and the initial line in the (ξ, η)-plane respectively. With (2.27), (2.19) and (2.22) we have the following boundary and initial conditions:

$$
u(\xi, \eta_{\mathrm{c}}(\xi)) = 0, \quad \psi(\xi, \eta_{\mathrm{c}}(\xi)) = 0
\tag{2.28}
$$

at the top of the cylinder;

$$u(\xi_p(\eta), \eta) = U_p(M\tau(\xi_p(\eta), \eta)), \quad \psi(\xi_p(\eta), \eta) = 1 \qquad (2.29\,a, b)$$

at the piston; and

$$\left.\begin{aligned}
u(\xi_i, \eta) &= u_i(\psi(\xi_i, \eta)), \\
P(\xi_i, \eta) &= 1 + \frac{\gamma - 1}{2} M P_i(\psi(\xi_i, \eta)) \quad \xi_i = \xi_i(\eta), \\
S(\xi_i, \eta) &= Y(\xi_i, \eta) = 1, \\
\tau(\xi_i, \eta) &= 0,
\end{aligned}\right\} \qquad (2.30)$$

on the initial line.

3. Gasdynamic perturbations in an inert gas

3.1. *Two-timescale asymptotic expansion*

Here we non-dimensionalize the time by $t'_a = t'_g$ from (2.5) using $u'_g = \max u'(x, 0)$, and allow for moderate rates of compression, such that the non-dimensional timescales are

$$t_g = t_p = 1, \quad t_s = M. \qquad (3.1)$$

In addition we set $r \equiv 0$ and $S \equiv 1$. Inspection of the compatibility equations $(2.26\,a, b)$ shows that it is essentially the small parameter

$$\delta = \frac{\gamma - 1}{2} M \qquad (3.2)$$

that dominates the relation between P and u in a pressure wave. Therefore we shall perform a perturbation analysis expanding all unknown functions in powers of δ, thereby employing the method of multiple scaling to account for the different characteristic times of piston motion and wave propagation. We set

$$F(\xi, \eta; \delta) = F^{(0)}(\xi, \eta, \sigma) + \delta F^{(1)}(\xi, \eta, \sigma) + \ldots, \qquad (3.3)$$

where $F = (u, P, \psi)$, and where the slowly varying argument σ is defined by

$$\sigma = \tfrac{1}{2}\delta(\xi + \eta). \qquad (3.4)$$

It may be expected that the slow piston motion will enforce a nearly homogeneous pressure rise, on which gasdynamic disturbances of $O(\delta)$ are superimposed. Thus it is reasonable to set

$$P = P_0(\sigma) + \delta P^{(1)}(\xi, \eta, \sigma) + \ldots. \qquad (3.5)$$

In addition, the principal freedom in the numbering of the characteristics is used to let

$$\psi^{(0)} = \tfrac{1}{2}(\xi - \eta) \equiv \psi_0(\xi, \eta). \qquad (3.6)$$

A crucial difficulty arises owing to the slow mean-field compression, which is illustrated by figure 3(*a*), showing the path of a pressure disturbance in the Lagrangian space. As a consequence of the overall compression the average speed of sound increases and the characteristics come closer and closer together, such that a progressively refined resolution in time is required. This can not be provided by a
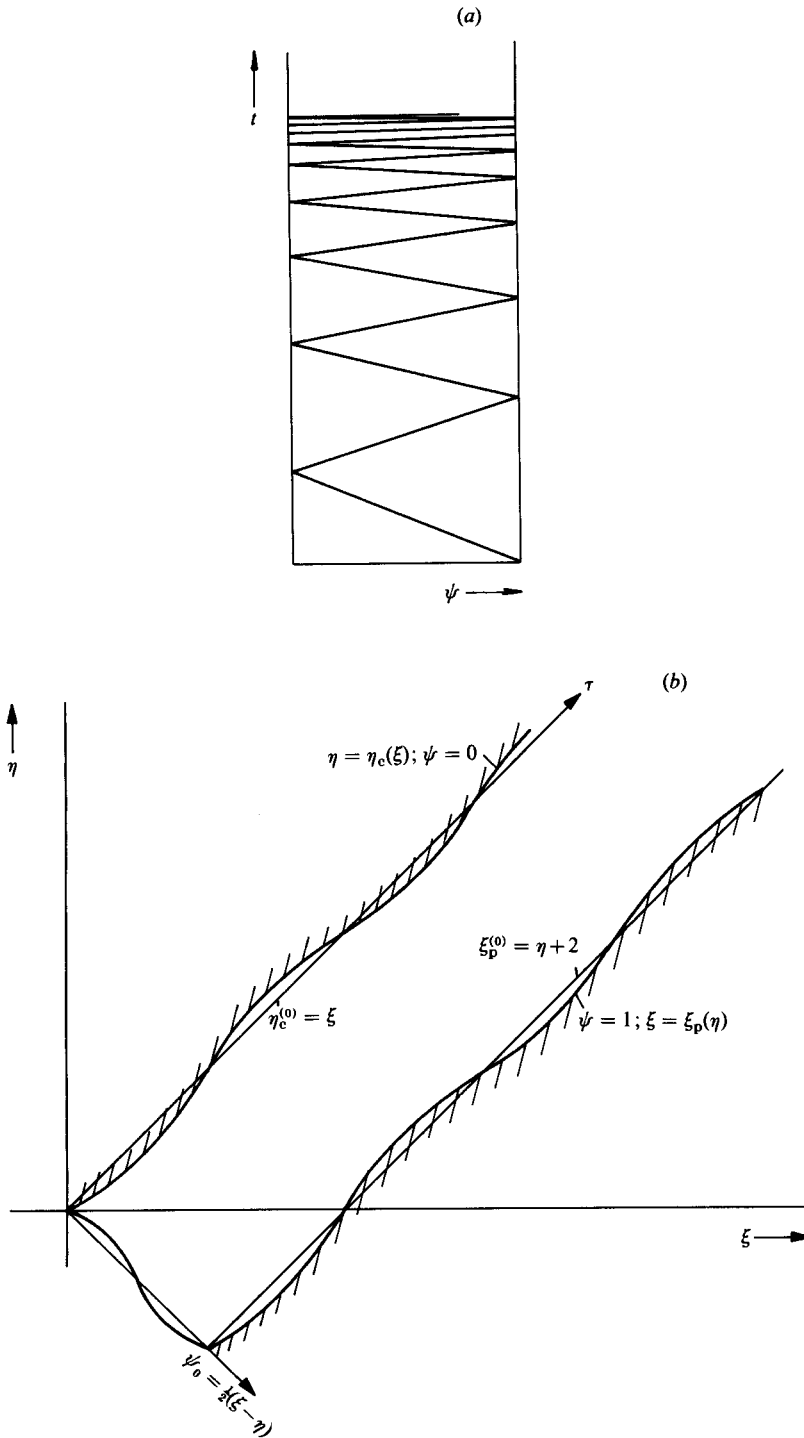
FIGURE 3. (a) The course of the characteristics in Lagrangian space, revealing the need for progressively refined temporal resolution after considerable overall compression. (b) The domains of integration in the characteristic space: ———, boundaries valid for the perturbation equations; ╱╱╱╱╱, boundaries valid for a particular solution of the model problem.

linearly stretched time coordinate expanded according to (3.3). However the expansion

$$\tau = \frac{1}{\delta} \int_0^{\sigma} P_0^{-\Gamma}(s)\, ds + \delta\tau^{(1)}(\xi, \eta, \sigma) + \dots \tag{3.7}$$

together with (3.6) ensures that to leading order the slope $(\partial\psi/\partial\tau)$ of the Mach characteristics is always adjusted to P^{Γ}, the slowly varying Lagrangian speed of sound, and it yields the desired refined resolution. A physical interpretation of the ratio σ/δ can be obtained by substituting $\psi = s/\delta$ in the integral in (3.7),

$$\tau = \int_0^{\sigma/\delta} \left| \frac{\partial\tau}{\partial\psi} \right|_{\pm}^{(0)} (\psi')\, d\psi' + \delta\tau^{(1)}. \tag{3.8}$$

This expression shows that σ/δ may be considered as the amount of mass that, to leading order, can be passed by an acoustic wave during the time τ. In addition, using (2.23), (3.2), (3.4) and (3.7) the slow time t can be related to σ by

$$t = t_0(\sigma) + O(\delta^2); \quad t_0(\sigma) = \frac{2}{\gamma - 1} \int_0^{\sigma} P_0^{-\Gamma}(s)\, ds. \tag{3.9}$$

With these perturbation expansions we finally obtain the following hierarchy of characteristic equations:

$$P_{\xi}^{(1)} + u_{\xi}^{(0)} = -\tfrac{1}{2}\dot{P}_0, \quad P_{\eta}^{(1)} - u_{\eta}^{(0)} = -\tfrac{1}{2}\dot{P}_0, \tag{3.10a}$$

$$P_{\xi}^{(2)} + u_{\xi}^{(1)} = -\tfrac{1}{2}(P_{\sigma}^{(1)} + u_{\sigma}^{(0)}), \quad P_{\eta}^{(2)} - u_{\eta}^{(1)} = -\tfrac{1}{2}(P_{\sigma}^{(1)} - u_{\sigma}^{(0)}), \tag{3.10b}$$

$$\psi_{\xi}^{(1)} - P_0^{\Gamma}\tau_{\xi}^{(1)} = +\tfrac{1}{2}\Gamma\frac{P^{(1)}}{P_0}, \quad \psi_{\eta}^{(1)} + P_0^{\Gamma}\tau_{\eta}^{(1)} = -\tfrac{1}{2}\Gamma\frac{P^{(1)}}{P_0}. \tag{3.10c}$$

Here the dot denotes the derivative with respect to σ.

These equations show the advantage of the Ansatz (3.6) and (3.7). There are no secular terms on the right-hand side of (3.10c) that contain the leading-order coordinate functions. Such terms had caused divergences in $\psi^{(1)}, \tau^{(1)}$ in the work of G. H. Schneider (1979). The boundary functions η_c, ξ_p are also expanded in the form

$$\left. \begin{aligned} \eta_c(\xi) &= \eta_c^{(0)}(\xi, \sigma) + \delta\eta_c^{(1)}(\xi, \sigma) + \dots, \\ \xi_p(\eta) &= \xi_p^{(0)}(\eta, \sigma) + \delta\xi_p^{(1)}(\eta, \sigma) + \dots, \end{aligned} \right\} \tag{3.11}$$

with $\sigma = \sigma(\xi, \eta_c(\xi))$ and $\sigma = \sigma(\xi_p(\eta), \eta)$, respectively. Equations (3.6) and (3.7) ensure that the leading-order terms $\eta_c^{(0)}, \xi_p^{(0)}$ become

$$\eta_c^{(0)}(\xi, \sigma) = \xi, \quad \xi_p^{(0)}(\eta, \sigma) = \eta + 2, \tag{3.12}$$

and thus do not depend on σ. By means of the expansions (3.11) one may transform the boundary conditions to the leading-order boundaries $\eta_c^{(0)}, \xi_p^{(0)}$ and thus obtain the domain of integration in the characteristic space, which is shown in figure 3(b). The boundaries, valid for the perturbation equations, are fixed by means of (3.12), whereas the actual boundaries $\eta = \eta_c(\xi)$ and $\xi = \xi_p(\eta)$, along which the relations $\psi = 0$ and $\psi = 1$ hold respectively, in general depend on the particular solutions. Therefore they cannot be calculated to a given order of approximation, before the hierarchy of equations of direction is solved up to the same order. Furthermore it is not possible to fix a scale of the τ-axis in the characteristic space *a priori*, since the resolution of the fast-time processes is automatically adjusted to the average

frequency of the wave reflections. The latter is determined by the bulk compression and therefore depends on the particular choice of the piston motion in any special solution of the problem.

It is especially important that $\eta_c^{(0)}$ and $\xi_p^{(0)}$ do not depend on σ, since in the later analysis we shall have to solve differential equations, which determine the derivatives $\partial F^{(i)}(\xi, \eta, \sigma)/\partial\sigma$, by means of integrations with respect to σ at constant (ξ, η). The non-dependence of the domain of integration in the (ξ, η)-space on σ then ensures that these integrations can be performed for all (ξ, η) within this domain and without restrictions on σ.

The transformation of the boundary conditions yields

$$u^{(0)}(\xi, \xi, \sigma) = 0, \tag{3.13a}$$

$$u^{(1)}(\xi, \xi, \sigma) = -u_\eta^{(0)}(\xi, \xi, \sigma)\,\eta_c^{(1)}(\xi, \sigma), \tag{3.13b}$$

$$\psi^{(1)}(\xi, \xi, \sigma) = \tfrac{1}{2}\eta_c^{(1)}(\xi, \sigma) \tag{3.13c}$$

at the top of the cylinder, and at the piston surface it yields

$$u^{(0)}(\eta + 2, \eta, \sigma) = U_p(t_0(\sigma)), \tag{3.14a}$$

$$u^{(1)}(\eta + 2, \eta, \sigma) = -u_\xi^{(0)}(\eta + 2, \eta, \sigma)\,\xi_p^{(1)}(\eta, \sigma), \tag{3.14b}$$

$$\psi^{(1)}(\eta + 2, \eta, \sigma) = -\tfrac{1}{2}\xi_p^{(1)}(\eta, \sigma). \tag{3.14c}$$

The initial conditions become

$$u^{(0)}(-\eta, \eta, 0) = u_i(-\eta), \tag{3.15a}$$

$$P_0(0) = 1, \tag{3.15b}$$

$$P^{(1)}(-\eta, \eta, 0) = P_i(-\eta), \tag{3.15c}$$

where we used $\psi_0(-\eta, \eta) = -\eta$.

3.2. First-order solutions and leading-order secular equations

Equations of compatibility along wave paths

Equation (3.10a) may be integrated along the characteristics to yield the general solutions

$$P^{(1)}(\xi, \eta, \sigma) = F(\xi, \sigma) + G(\eta, \sigma), \tag{3.16a}$$

$$u^{(0)}(\xi, \eta, \sigma) = -\tfrac{1}{2}(\xi - \eta)\dot{P}_0(\sigma) - F(\xi, \sigma) + G(\eta, \sigma). \tag{3.16b}$$

The boundary condition (3.13a) gives

$$G(\xi, \sigma) = F(\xi, \sigma) \tag{3.17a}$$

and hence

$$P^{(1)}(\xi, \eta, \sigma) = F(\xi, \sigma) + F(\eta, \sigma), \tag{3.17b}$$

whereas (3.14a) then yields a recursion relation for F

$$F(\eta, \sigma) = F(\eta + 2, \sigma) + (U_p(t_0(\sigma)) + \dot{P}_0(\sigma)). \tag{3.18}$$

Using (3.16a) for $P^{(1)}$, this relation can be written as

$$\dot{P}_0(\sigma)\,\Delta\sigma + \delta(P^{(1)}(\xi + 2, \eta + 2, \sigma) - P^{(1)}(\xi, \eta, \sigma)) = -U_p(t_0(\sigma))\,\Delta\sigma, \tag{3.19}$$

where $\Delta\sigma = \sigma(\xi + 2, \eta + 2, \delta) - \sigma(\xi, \eta, \delta) = 2\delta$ is the difference in σ between $(\xi + 2, \eta + 2)$ and (ξ, η) (cf. figure 9).

The left-hand side of (3.19) is the net change of P to $O(\delta)$, and it is related to the mean compression due to the piston motion, which is represented by the right-hand side. In order to obtain a uniformly valid approximation, the successive expansion functions $F^{(i)}$, $F^{(i+1)}$ are required to be of the same order of magnitude. Since δ in (3.4) is arbitrary, σ can be fixed independent of ξ and η. Thus the pressure rise in (3.19) is to be distributed between $\dot{P}_0 \Delta\sigma$ and the difference $P^{(1)}(\xi+2, \eta+2, \sigma) - P^{(1)}(\xi, \eta, \sigma)$ such that $P^{(1)}$ remains bounded for all allowed (ξ, η). Applying (3.19) n times, one obtains the first-order pressure difference

$$P^{(1)}(\xi+2n, \eta+2n, \sigma) - P^{(1)}(\xi, \eta, \sigma) = -2n[U_\mathrm{p}(t_0(\sigma)) + \dot{P}_0(\sigma)]. \tag{3.20}$$

Since n may be arbitrarily large, $P^{(1)}$ is bounded everywhere only if the right-hand side of (3.20) vanishes identically. This requirement represents a secular equation for the slow-time variation of the pressure function $P_0(\sigma)$,

$$\dot{P}_0(\sigma) = -U_\mathrm{p}(t_0(\sigma)), \tag{3.21}$$

where $t_0(\sigma)$ is taken from (3.9). Thus (3.18) leads to

$$F(\xi, \sigma) = F(\xi+2, \sigma), \tag{3.22}$$

indicating that F must have period two with respect to ξ. Since $P = T^{\frac{1}{2}} = p^{\frac{\gamma-1}{2\gamma}}$, with the aid of (3.9) and with $U_\mathrm{p} = \mathrm{d}X_\mathrm{p}/\mathrm{d}t$ one finally obtains

$$(pX_\mathrm{p}^\gamma)^{(0)} \equiv 1 \tag{3.23}$$

from (3.21). Since in our closed piston–cylinder system X_p is proportional to the specific volume, this equation shows that the accumulation of the weak pressure waves leads to the bulk pressure rise given by the law of adiabatic compression of an inert gas. This result was already obtained by G. H. Schneider (1979).

Equations of direction

Equations (3.10c) may formally be integrated. However, in the boundary conditions (3.13) and (3.14), the boundary functions $\eta_\mathrm{c}^{(1)}(\eta, \sigma), \eta_\mathrm{p}^{(1)}(\xi, \sigma)$ appear, which are still undetermined. Thus at this stage it is not possible to calculate the integration functions ν, μ appearing in the general solutions

$$\psi^{(1)} - P_0^\Gamma \tau^{(1)} = \frac{\Gamma}{2P_0(\sigma)} \int_\eta^\xi P^{(1)}(\zeta, \eta, \sigma) \, \mathrm{d}\zeta + \nu(\eta, \sigma), \tag{3.24a}$$

$$\psi^{(1)} + P_0^\Gamma \tau^{(1)} = \frac{-\Gamma}{2P_0(\sigma)} \int_{\xi-2}^\eta P^{(1)}(\xi, \zeta, \sigma) \, \mathrm{d}\zeta + \mu(\xi, \sigma). \tag{3.24b}$$

With the aid of (3.17b), $\psi^{(1)}$ and $\tau^{(1)}$ become

$$\psi^{(1)}(\xi, \eta, \sigma) = \frac{\Gamma}{2P_0} \Bigg[\psi_0(\xi, \eta) \, (F(\xi, \sigma) + F(\eta, \sigma)) - F(\xi, \sigma)$$

$$+ \frac{1}{2} \int_\eta^\xi F(\zeta, \sigma) \, \mathrm{d}\zeta - \frac{1}{2} \int_{\xi-2}^\eta F(\zeta, \sigma) \, \mathrm{d}\zeta \Bigg] + \tfrac{1}{2}(\mu(\xi, \sigma) + \nu(\eta, \sigma)), \tag{3.25a}$$

$$P_0^\Gamma \tau^{(1)}(\xi, \eta, \sigma) = \frac{\Gamma}{2P_0} [\psi_0(\xi, \eta) \, (F(\xi, \sigma) - F(\eta, \sigma)) - F(\xi, \sigma) - \bar{F}(\sigma)]$$

$$+ \tfrac{1}{2}[\mu(\xi, \sigma) - \nu(\eta, \sigma)]. \tag{3.25b}$$

The boundary functions are then

$$\eta_{\mathrm{c}}^{(1)}(\xi, \sigma) = -\frac{\Gamma}{P_0(\sigma)} [F(\xi, \sigma) + \bar{F}(\sigma)] + [\mu(\xi, \sigma) + \nu(\xi, \sigma)], \qquad (3.26a)$$

$$\xi_{\mathrm{p}}^{(1)}(\eta, \sigma) = -\frac{\Gamma}{P_0(\sigma)} [F(\eta, \sigma) + \bar{F}(\sigma)] - [\mu(\eta + 2, \sigma) + \nu(\eta, \sigma)], \qquad (3.26b)$$

where we used (3.13c) and (3.14c), and where

$$\bar{F}(\sigma) = \frac{1}{2} \int_{-1}^{1} F(\zeta, \sigma) \, \mathrm{d}\zeta. \qquad (3.27)$$

Anticipating the secular equation (3.39) for F and using (3.16b) and (3.22), it can be shown that the expression $\frac{1}{2}[\eta_{\mathrm{c}}^{(1)}(\xi, \sigma) + \xi_{\mathrm{p}}^{(1)}(\xi, \sigma)]$ must have period two in ξ, as all other terms in that equation. With (3.26) this results in

$$\Delta\mu(\xi, \sigma) \equiv \mu(\xi + 2, \sigma) - \mu(\xi, \sigma) = \mu(\xi + 4, \sigma) - \mu(\xi + 2, \sigma) = \dots,$$

such that the functional form of μ is

$$\left.\begin{aligned} \mu(\xi, \sigma) &= \mu^*(\xi^*, \sigma) + K(\xi)\,\Delta\mu(\xi^*, \sigma), \\ \xi^* &= \xi - 2K(\xi), \end{aligned}\right\} \quad (-1 < \xi^* < 1). \qquad (3.28)$$

The K-function is defined as

$$K(\xi) = \sum_{i=0}^{\infty} H[\xi - (2i + 1)]. \qquad (3.29)$$

Here H is the Heaviside step function

$$H(\xi) = \begin{cases} 0 & (\xi < 0), \\ 1 & (\xi > 0). \end{cases} \qquad (3.30)$$

Furthermore the requirement $\psi^{(1)} = O(\psi_0) = O(1)$ must hold, and therefore

$$\mu^*(\xi^*, \sigma) + K(\xi)\,\Delta\mu(\xi^*, \sigma) + \nu(\eta, \sigma) = O(1). \qquad (3.31)$$

Since ξ^* and η vary independently, the second and third terms in general cannot sum up to $O(1)$ and one has to require

$$\Delta\mu^* \equiv 0 \quad \text{or} \quad \mu(\xi, \sigma) = \mu^*(\xi^*, \sigma) = O(1) \qquad (3.32)$$

and

$$\nu(\eta, \sigma) = \nu^*(\eta, \sigma) = O(1). \qquad (3.33)$$

This ensures that both $\psi^{(1)}$ and $\tau^{(1)}$ remain $O(1)$, and that divergences in $\psi^{(2)}$, $\tau^{(2)}$ are avoided, as can be seen in a second-order expansion of the equations of direction.

A special result obtained from (3.26) is

$$\tfrac{1}{2}[\eta_{\mathrm{c}}^{(1)}(\xi, \sigma) + \xi_{\mathrm{p}}^{(1)}(\xi, \sigma)] = \frac{-\Gamma}{P_0(\sigma)} [F(\xi, \sigma) + \bar{F}(\sigma)], \qquad (3.34)$$

which by means of (3.39) shows that the functions μ^* and ν^* do not affect the development of the wave profile function F. Furthermore they merely correspond to $O(M^2)$-corrections to the slow time $t = M\tau$. Since we are interested in $O(1)$-changes of the evolution of the ignition process we will not examine additional constraints on μ^*, ν^* here.

3.3. *Second-order solutions and secular equations for the first-order functions*
Equations of compatibility along wave path

Some details of the following derivations can be found in Appendix B. The general solutions for $P^{(2)}$ and $u^{(1)}$, obtained from integrations of (3.10b), are

$$P^{(2)}(\xi,\eta,\sigma) = \tfrac{1}{2}\ddot{P}_0(\sigma)\,(\psi_0^2(\xi,\eta)-\tfrac{1}{2})+\psi_0(\xi,\eta)\,[F_\sigma(\xi,\sigma)-F_\sigma(\eta,\sigma)]$$
$$-F_\sigma(\xi,\sigma)+F^{(2)}(\xi,\sigma)+G^{(2)}(\eta,\sigma), \quad (3.35a)$$

$$u^{(1)}(\xi,\eta,\sigma) = \tfrac{1}{4}\ddot{P}_0(\sigma)-\psi_0(\xi,\eta)\,[F_\sigma(\xi,\sigma)+F_\sigma(\eta,\sigma)]$$
$$+F_\sigma(\xi,\sigma)-F^{(2)}(\xi,\sigma)+G^{(2)}(\eta,\sigma). \quad (3.35b)$$

The same steps that led to the recursion formula for F give a similar relation for $F^{(2)}$. The requirement
$$P^{(2)} = O(P^{(1)}) = O(1) \tag{3.36}$$

for all allowed (ξ,η,σ) results in a secular equation for $P^{(1)}$ and $F(\xi,\sigma)$. With the definitions

$$u_c^{(1)}(\xi,\sigma) \equiv -u_\eta^{(0)}(\xi,\xi,\sigma)\,\eta_c^{(1)}(\xi,\sigma), \tag{3.37a}$$

$$u_p^{(1)}(\eta,\sigma) \equiv -u_\xi^{(0)}(\eta+2,\eta,\sigma)\,\xi_p^{(1)}(\eta,\sigma), \tag{3.37b}$$

one may write the secular equation for $P^{(1)}$ in the form

$$P_\sigma^{(1)}(\xi,\eta,\sigma) = \tfrac{1}{2}(u_c^{(1)}(\xi,\sigma)+u_c^{(1)}(\eta,\sigma))-\tfrac{1}{2}(u_p^{(1)}(\xi,\sigma)+u_p^{(1)}(\eta,\sigma)). \tag{3.38}$$

The right-hand side, containing $u_p^{(1)}, u_c^{(1)}$, is a correction to the first-order approximation, which prescribed the velocities $u^{(0)} = 0$ and $u^{(0)} = U_p$ at $\psi_0 = 0$ and $\psi_0 = 1$ instead of $\psi = 0$ and $\psi = 1$.

It is seen that the first-order velocities at the boundaries determine the slow-timescale variation of $P^{(1)}$ in the same way as the piston motion caused the mean-field pressure changes by means of (3.21). The secular equation for $F(\xi,\sigma)$ is obtained from (3.38), collecting all terms on the right-hand side that only depend on ξ and σ. With the aid of (3.37), (3.16) and (3.17) one finds

$$F_\sigma(\xi,\sigma) = -u_\eta^{(0)}(\xi+2,\xi,\sigma)\tfrac{1}{2}(\eta_c^{(1)}(\xi,\sigma)+\xi_p^{(1)}(\xi,\sigma)). \tag{3.39}$$

Additional use of (3.34) yields a closed-form equation for $F_\sigma(\xi,\sigma)$,

$$F_\sigma(\xi,\sigma) = \frac{\Gamma}{P_0(\sigma)}(\tfrac{1}{2}\dot{P}_0(\sigma)+F_\xi(\xi,\sigma))\,(F(\xi,\sigma)+\bar{F}(\sigma)). \tag{3.40}$$

The initial conditions for $F(\xi,\sigma)$ follow from those for $P^{(1)}$ and $u^{(0)}$, (3.15), and from the general solutions, (3.16) and (3.17),

$$F(\xi,0) = \begin{cases} \tfrac{1}{2}[P_i(\xi)-(u_i(\xi)-\xi U_p(0))] & (0 < \xi \leqslant 1), \\ \tfrac{1}{2}[P_i(-\xi)+(u_i(-\xi)+\xi U_p(0))] & (-1 < \xi \leqslant 0). \end{cases} \tag{3.41}$$

Once solutions to (3.40) and (3.41) are known, the first-order approximation is completed except for the coordinate integration functions μ^*, ν^*.

3.4. *Wave deformation and shock formation time*
The first-order pressure function $P^{(1)}$ is composed of two contributions, each depending on either (ξ,σ) or (η,σ) as can be seen from (3.16) and (3.17). This may be interpreted as the superposition of two wave trains travelling in opposite directions

and having the same profile function $F(\xi, \sigma)$. The secular equation (3.40) for F describes the deformation of the waves with increasing time. Note, that with this relation the nonlinear structure of the system is retained. In particular, the development of multivalued regions in the (ξ, σ)-plane indicates shock formation.

Equation (3.40) can be written in characteristic form as

$$\left(\frac{\partial F}{\partial \sigma}\right)_c = F_\sigma + A[F; \sigma] F_\xi = \frac{\Gamma \dot{P}_0}{2 P_0} (F + \bar{F}). \tag{3.42}$$

Here c denotes the characteristics of (3.42), whose directions in the (ξ, σ)-space are given by

$$\left(\frac{\partial \xi}{\partial \sigma}\right)_c = A[F; \sigma] = -\frac{\Gamma}{P_0(\sigma)} (F + \bar{F}). \tag{3.43}$$

Notice that (3.42) is an integro–differential equation and $A(F; \sigma)$ is a functional depending on all values of F in $-1 < \xi \leqslant 1$ for constant σ. In terms of characteristic coordinates of (3.42), namely

$$(c, \sigma) = (c(\xi, \sigma), \sigma), \tag{3.44}$$

multivalued regions in the (ξ, σ)-space are indicated by

$$b(c, \sigma) \equiv \frac{\partial \xi(c, \sigma)}{\partial c} = 0, \tag{3.45}$$

since in that case two characteristics labelled by c and $c + \mathrm{d}c$ cross each other. If $b(c, \sigma)$ is known (3.45) can be considered as an implicit relation $\sigma_\mathrm{sh} = \sigma_\mathrm{sh}(c)$, and the minimum of this function determines the slow-scale shock formation time t_sh up to first order via

$$t_\mathrm{sh} = \frac{2}{\gamma - 1} \int_0^{\sigma_\mathrm{sh}} P_0^{-\Gamma}(s) \, \mathrm{d}s + O(M\delta). \tag{3.46}$$

Differentiation of (3.42) and (3.43) with respect to c gives

$$\frac{\partial}{\partial \sigma} \left(\frac{\partial F}{\partial c}\right) = \frac{\Gamma}{2} \frac{\mathrm{d} \ln P_0}{\mathrm{d}\sigma} \frac{\partial F}{\partial c}, \tag{3.47}$$

$$\frac{\partial}{\partial \sigma} (b) = -\frac{\Gamma}{P_0} \frac{\partial F}{\partial c}, \tag{3.48}$$

where the derivatives refer to (c, σ) as the set of independent variables. First, (3.47) is solved by

$$\frac{\partial F}{\partial c} = \left(\frac{\partial F(\xi, \sigma)}{\partial \xi}\right)_{(\xi=c, \sigma=0)} P_0^{\Gamma/2}(\sigma) \equiv F_{\xi 0}(c) P_0^{\Gamma/2}(\sigma), \tag{3.49}$$

and then (3.48) is integrated to give

$$b(c, \sigma) = 1 - \Gamma F_{\xi 0}(c) \int_0^\sigma P_0^{\Gamma/2 - 1}(s) \, \mathrm{d}s. \tag{3.50}$$

Thus the relation for σ_sh is

$$\int_0^{\sigma_\mathrm{sh}} P_0^{\Gamma/2 - 1}(s) \, \mathrm{d}s = \frac{1}{\Gamma \max(F_\xi(\xi, 0))} \tag{3.51}$$

if there is at least a small interval where $F_\xi(\xi, 0) > 0$.

On the other hand, those characteristics that have $F_{\xi 0}(c) < 0$ spread out in time, as is suggested by the fact that $b(c, \sigma) = \partial \xi / \partial c$ then grows monotonically with σ. An

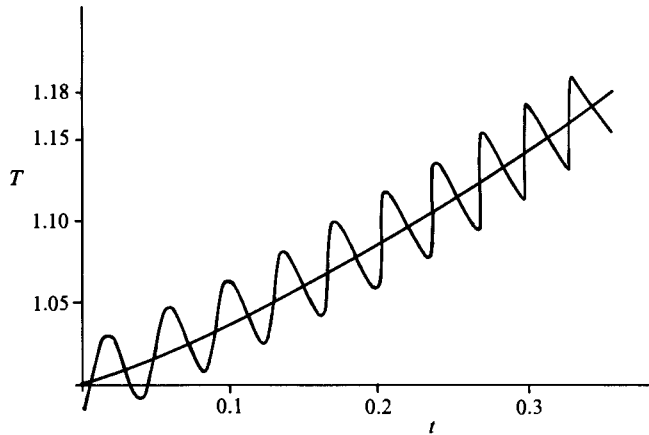FIGURE 4. The steepening of an initially smooth wave and shock formation, represented by the temperature at the piston surface.

increasing value of b means that an interval $d\xi(\sigma)$, which at 'time' σ covers the characteristics coming from an initial interval dc, broadens with time. In figure 4 we have plotted the temperature at the piston surface versus time, for the case of a sinusoidal initial disturbance. (This is convenient, since $T = P^2$ follows from (2.20b) if $S \equiv 1$.) The steepening of the wave front up to shock formation and the corresponding flattening of the wave tails is obvious. These effects are both related to the properties of $b(c, \sigma)$ mentioned above. For more details concerning the numerical evaluations, see §5.

3.5. *Special solutions for an initially undisturbed gas*

For initial conditions with the gas at rest and with an impulsive start of the piston motion, the initial conditions (3.41) for F reduce to

$$F(\xi, 0) = \tfrac{1}{2}\xi U_p(0) \quad (-1 < \xi < 1). \tag{3.52}$$

Separation of variables according to

$$F(\xi, \sigma) = \Theta(\sigma)\, \Xi(\xi) \tag{3.53}$$

together with (3.52) leads to the solution

$$\dot{F}(\xi, \sigma) = -\frac{P_0^{\Gamma/2}(\sigma)}{\left(\dfrac{2}{\dot{P_0}(0)} + \Gamma \displaystyle\int_0^\sigma P_0^{\Gamma/2-1}(s)\,\mathrm{d}s\right)}(\xi - 2K(\xi)). \tag{3.54}$$

For the case of constant piston speed, say $U_p = -1$, the exact solution is known. There is one shock reflected repeatedly between the piston and the top of the cylinder separating two homogeneous regions, one region with constant velocity $u = U_p$ and the other with the gas at rest. The pressure rise across the shocks is given by Rankine–Hugoniot's law, which to first order in the shock strength can be written as (Seifert 1962; Whitham 1974)

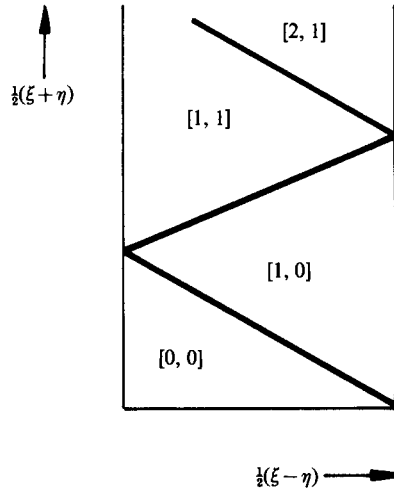$$[P] = \pm M \frac{\gamma - 1}{2}[u]. \tag{3.55}$$

FIGURE 5. Domains of constant pressure and velocity when shocks are initiated by an impulsive start of the piston motion and when the piston speed is constant.
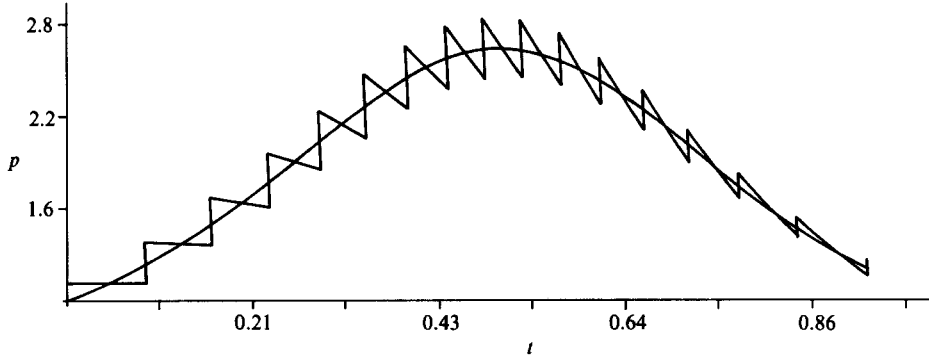

FIGURE 6. Decay of the shock strength after multiple reflections for a periodic piston motion.

Evaluation of (3.21) for P_0 and of (3.54) yield

$$P_0(\sigma) = 1 + \sigma, \tag{3.56}$$

and
$$F(\xi, \sigma) = -\tfrac{1}{2}[\xi - 2K(\xi)] \quad (\xi > -1). \tag{3.57}$$

Replacing σ by $\tfrac{1}{2}\delta(\xi + \eta)$, it is seen how the change of $P^{(1)}$ between the passage of two shocks compensates the slow change of P_0. The solution, up to and including first order, for P is

$$P(\xi, \eta) = 1 + \frac{\gamma - 1}{2}M[K(\xi) + K(\eta)] + O(\delta^2), \tag{3.58}$$

and to leading order for u we have

$$u(\xi, \eta) = -[K(\xi) - K(\eta)] + O(\delta). \tag{3.59}$$

As shown in figure 5 the region $\xi - 2 < \eta < \xi$ in the (ξ, η)-plane is divided into triangles, each corresponding to a pair $[K(\xi), K(\eta)]$, in which there are constant
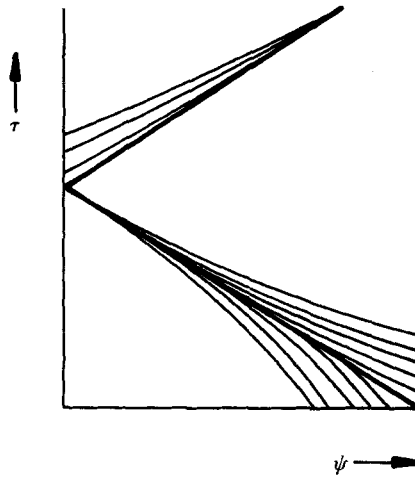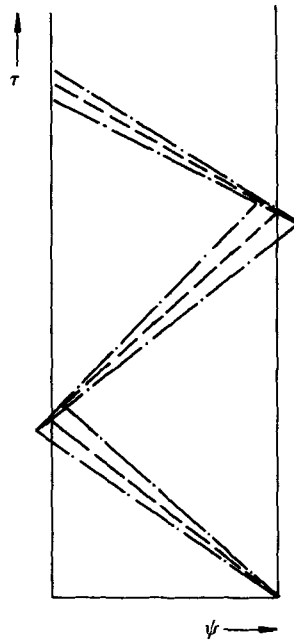
Figure 7. Characteristics crossing the path of the shock.

Figure 8. Multivalued regions in the Lagrangian space indicating the presence of shocks; ·—·—·—, bounding characteristics of the multivated regions; ————, shock lines.

values of pressure and velocity. Where $K(\xi) - K(\eta) = 1$ we have $u = -1 + O(\delta)$, while where $K(\xi) - K(\eta) = 0$ it is $u = O(\delta)$. The pressure function changes through

$$[P] = M\frac{\gamma-1}{2} + O(M^2) = \pm M\frac{\gamma-1}{2}[u] + O(M^2)$$

at each discontinuity, as required above.

As a second example we have considered a periodic piston motion given by

$$U_p(t) = -\tfrac{1}{2}\pi \cos(\pi t). \tag{3.60}$$

Figure 6 shows the pressure p versus time, as it comes out of an evaluation of (3.54). It is seen that the shock strength continuously decreases. This is a consequence of the growth of the integral in the denominator in (3.54). As is depicted in figure 7, this decay of the wave amplitudes can be explained physically as the result of expansion waves starting from the piston, when it is decelerated, overtaking the shock and weakening it. More generally, this effect is expressed in (3.38), where the first-order velocity corrections $u_c^{(1)}$, $u_p^{(1)}$ at the boundaries enter into the secular equation for $P^{(1)}$.

Figure 8 qualitatively shows the multivalued regions in the Lagrangian space obtained by formal evaluations of the solutions for $\psi^{(1)}$ and $\tau^{(1)}$. These regions have to be replaced by shocks in order to construct physically meaningful solutions. Setting $(\psi_{sh}, \tau_{sh}) = \frac{1}{2}(\psi^+ + \psi^-, \tau^+ + \tau^-)$, where $\psi^\pm, \tau^\pm$ denote the first-order approximations to ψ and τ at the boundaries of the multivalued regions, we are in agreement with the bisector rule for weak shock propagation described by Kluwick (1981) and W. Schneider (1978).

4. Reactive gas

In this section the reference time t_a' is identified with the ignition delay time t_I', such that $t_I \equiv 1$. Before entering into the details of the analysis, an *a priori* estimate of the effects of the disturbances and of the mean-field compression on the reaction rate will be performed. Expanding the right-hand side of (2.18c) with respect to δ one obtains

$$(-\Delta h)\, r = \frac{1}{\gamma} Y^{(0)} \exp\left[\frac{1}{\epsilon}\left(1 - \frac{1}{T^{(0)}}\right)\right] \exp\left[\frac{\delta}{\epsilon}\frac{T^{(1)}}{T^{(0)2}} + O\left(\frac{\delta^2}{\epsilon}\right)\right]. \tag{4.1}$$

Owing to the factor of $1/\epsilon$ in the first exponential, an $O(1)$ deviation of the mean-field temperature $T^{(0)}$ above unity immediately leads to an exponentially large reaction rate. In this case there is no longer an induction phase precursing ignition, but the whole process is driven by the compression. We therefore require that all the bulk quantities may only change about $O(\epsilon)$ on the ignition timescale. This is equivalent to setting

$$X_p(t) = 1 - \epsilon v(t), \quad \rho(t) = 1 + \epsilon v(t) + \dots, \tag{4.2}$$

and thus treating the deviations of bulk quantities from their initial values as perturbations. From (4.2) we conclude $U_p(t) = O(\epsilon)$ in this regime, which confirms (2.13). On the other hand, it is seen from the second exponential in (4.1) that the gasdynamic disturbances enforce $O(1)$-changes of the reaction rate only if $\delta = \frac{1}{2}M(\gamma - 1) = O(\epsilon)$, as was anticipated in §2 as well.

4.1. *Ignition under homogeneous compression*

Based on (4.2) one may estimate $u = O(U_p) = O(\epsilon)$, which implies $p = p(t)$ by means of (2.18b). Using $p = \rho T$, the equations for temperature and fuel mass fraction can then be transformed to

$$T_t - \epsilon(\gamma - 1)\, T\dot{v} = \epsilon\gamma(-\Delta h)\, r + O(\epsilon^2), \quad Y_t = -\epsilon r. \tag{4.3a,b}$$

The dependent variables T, Y are expanded in powers of ϵ as

$$\left.\begin{array}{l} T = 1 + \epsilon T^{(1)} + O(\epsilon^2), \\ Y = 1 + O(\epsilon). \end{array}\right\} \tag{4.4}$$

Insertion into the energy equation (4.3a) yields

$$T_t^{(1)} - (\gamma - 1)\dot{v}(t) = \gamma(-\Delta h)\, r^{(0)} = \exp(T^{(1)}) \tag{4.5}$$

(cf. (4.1) with $\delta = \epsilon$ and $T^{(0)} = Y^{(0)} \equiv 1$).

The solution is subject to the initial condition

$$T^{(1)}(0) = 0. \tag{4.6}$$

Equation (4.5) is solved explicitly by means of the transformation $\phi(t) = \exp(-T^{(1)})$, with $\phi(0) = 1$, and amounts to

$$T^{(1)}(t) = (\gamma - 1)v(t) - \ln\left(1 - \int_0^t \exp((\gamma - 1)v(s))\, \mathrm{d}s\right). \tag{4.7}$$

For $v \equiv 0$ we obtain Frank–Kamenetskii's result

$$T^{(1)}(t) = -\ln(1 - t). \tag{4.8}$$

Since we have scaled the time with t_I' from (2.2), it is seen that the ignition delay time t_I' indeed represents the time to ignition under constant density conditions.

Requiring $T^{(1)} \to \infty$ the time to ignition $t_{I,v}$ for slow compression is obtained from the condition

$$\int_0^{t_{I,v}} \exp((\gamma - 1)\, v(s))\, \mathrm{d}s = 1. \tag{4.9}$$

This equation shows how a compression with $v(s) > 0$ accelerates the ignition process, while an expansion with $v(s) < 0$ slows it down.

4.2. Gasdynamic-chemical interactions

In addition to the mean-field compression, we now allow for gasdynamic perturbations, and introduce the distinguished limit

$$\frac{\delta}{\epsilon} = \omega = O(1), \quad \epsilon \to 0. \tag{4.10}$$

In the characteristic formulation, first-order variations of the entropy function and fuel mass fraction owing to the chemical reactions are prescribed by the compatibility relations along particle paths $\psi = \text{const.}$ It is convenient to introduce the new set of coordinates

$$(\psi_0, \phi, \sigma) = (\tfrac{1}{2}(\xi - \eta), \tfrac{1}{2}(\xi + \eta), \sigma) \tag{4.11}$$

for S and Y. Solutions of the form

$$\left.\begin{aligned} S &= 1 + \delta S^{(1)}(\psi_0, \phi, \sigma) + O(\delta^2), \\ Y &= 1 + O(\delta), \end{aligned}\right\} \tag{4.12}$$

are then expected. As in §4.1 it is not necessary to examine higher orders of Y if one is interested in thermal runaway only. Thus we consider an expansion of the energy equation (2.26c),

$$S_\phi^{(1)} = 0, \quad S^{(1)} = S^{(1)}(\psi_0, \sigma), \tag{4.13}$$

$$S_\phi^{(2)} = \psi_\phi^{(1)} S_{\psi_0}^{(1)} - S_\sigma^{(1)} + (-\Delta h)\frac{r^{(0)}}{(\gamma - 1)\,\omega}. \tag{4.14}$$

(A detailed expansion of the operator $\partial/\partial\tau$ along $\psi = \text{const.}$ in terms of derivatives with respect to (ψ_0, ϕ, σ) is given in Appendix C.)

With $r^{(0)}$ from (4.5), and by means of an expansion of the relation $T = S^2 P^2$, $r^{(0)}$ is expressed in terms of $S^{(1)}$, $P^{(1)}$ as

$$(-\Delta h)\, r^{(0)} = \frac{1}{\gamma} \exp\left[2\omega(S^{(1)} + P^{(1)})\right]. \tag{4.15}$$

Integration of (4.14) along $\psi_0 = \text{const.}$, from ϕ to $\phi + \Delta\phi$, yields

$$\Delta S^{(2)} = \Delta \psi^{(1)} S^{(1)}_{\psi_0} - \Delta\phi S^{(1)}_\sigma + \int_\phi^{\phi+\Delta\phi} \frac{(-\Delta h)}{(\gamma-1)\,\omega} r^{(0)} \, \mathrm{d}\phi. \tag{4.16}$$

Here $\Delta S^{(2)}$ and $\Delta \psi^{(1)} S^{(1)}_{\psi_0}$ are bounded for arbitrary $\Delta\phi$, such that the other two terms must balance each other. This gives the secular equation

$$S^{(1)}_\sigma = \frac{1}{2} \int_\phi^{\phi+2} \frac{(-\Delta h)}{(\gamma-1)\,\omega} r^{(0)}(S^{(1)}, P^{(1)}) \, \mathrm{d}\phi, \tag{4.17}$$

where we set $\Delta\phi = 2$, since $r^{(0)}$ has period 2 in ϕ via the periodicity of $P^{(1)}$ (cf. (3.16a), (3.17a) and (3.22)).

Since the time to ignition will be $O(1)$, while the characteristic time of the piston motion is $O(1/\epsilon)$ as in §4.1, the pressure function P is constant to leading order. Thus an appropriate expansion of P is

$$P = 1 + \delta P^{(1)}(\xi, \eta, \sigma) + \dots. \tag{4.18}$$

For τ this means, according to (3.7),

$$\tau = \tfrac{1}{2}(\xi + \eta) + \delta \tau^{(1)}(\xi, \eta, \sigma) + \dots. \tag{4.19}$$

Employing the notation of (4.2) for the piston motion, the boundary condition for u at $\psi = 1$, (2.29a), changes into

$$u(\xi_\mathrm{p}(\eta), \eta) = -\delta \dot{v}[M\tau(\xi_\mathrm{p}(\eta), \eta)]. \tag{4.20}$$

Thus in analogy with (3.13a), (3.14b) and using (3.37b), one has

$$\left.\begin{aligned} u^{(0)}(\eta+2, \eta, \sigma) &= 0, \\ u^{(1)}(\eta+2, \eta, \sigma) &= u^{(1)}_\mathrm{p}(\eta, \sigma) - \dot{v}(t_0(\sigma)). \end{aligned}\right\} \tag{4.21}$$
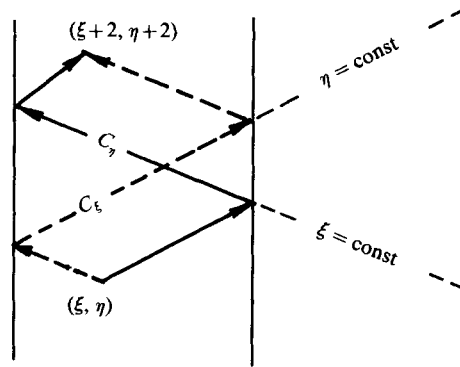
With $P_0 = 1$, $S = 1 + \delta S^{(1)}$, $r = r^{(0)}(S^{(1)}, P^{(1)}) + O(\delta)$, the compatibility relations along wave paths to first and second order change to

$$\left.\begin{aligned} P^{(1)}_\xi + u^{(0)}_\xi &= 0, \\ P^{(2)}_\xi + u^{(1)}_\xi &= \frac{-\Delta h}{2\omega} r^{(0)} + u^{(0)}_\xi S^{(1)} - \tfrac{1}{2}(P^{(1)}_\sigma + u^{(0)}_\sigma), \\ P^{(1)}_\eta - u^{(0)}_\eta &= 0, \\ P^{(2)}_\eta - u^{(1)}_\eta &= \frac{-\Delta h}{2\omega} r^{(0)} - u^{(0)}_\eta S^{(1)} - \tfrac{1}{2}(P^{(1)}_\sigma - u^{(0)}_\sigma). \end{aligned}\right\} \tag{4.22}$$

By the method described in §3 we finally obtain the following secular equation:

$$P^{(1)}_\sigma(\xi, \eta, \sigma) = \tfrac{1}{2}[u^{(1)}_\mathrm{c}(\xi, \sigma) + u^{(1)}_\mathrm{c}(\eta, \sigma)] - \tfrac{1}{2}[u^{(1)}_\mathrm{p}(\xi, \sigma) + u^{(1)}_\mathrm{p}(\eta, \sigma)]$$
$$+ \dot{v}(t_0(\sigma)) + \frac{1}{4} \int_{C_\xi + C_\eta} \left(\frac{-\Delta h}{2\omega} r^{(0)} - u^{(0)}_\eta S^{(1)}\right) \mathrm{d}\zeta. \tag{4.23}$$

The paths of integration C_ξ, C_η are shown in figure 9.

FIGURE 9. The paths of integration C_ξ, C_η.

The second term of the integrand results from the deviation of S from unity on the left-hand side of (2.26), while the integral over the source term $(-\Delta h) r^{(0)}$ represents an accumulation of second-order pressure waves along the Mach characteristics. These waves are initiated by thermal expansion due to the chemical heat release and, since $r^{(0)} = r^{(0)}(S^{(1)}, P^{(1)})$, there is an obvious feedback of the pressure perturbations via these chemically induced second-order wavelets. The process of self-heating within a particle is described by the secular equation (4.17), where the source term is integrated along a particle path not counting the deviation $\delta\psi^{(1)} + O(\delta^2)$.

From (4.23) one obtains an equation for the profile function

$$F_\sigma(\xi, \sigma) = \Gamma F_\xi(\xi, \sigma)\,(F(\xi, \sigma) + \bar{F}(\sigma)) + \tfrac{1}{2}\dot{v}(t_0(\sigma))$$

$$+ \frac{1}{4}\frac{(-\Delta h)}{2\omega} \int_\xi^{\xi+2} (r^{(0)}(\xi+2, \zeta, \sigma) + r^{(0)}(\zeta, \xi, \sigma))\,\mathrm{d}\zeta$$

$$- \frac{1}{4} \int_\xi^{\xi+2} F_\zeta(\zeta, \sigma)\,[S^{(1)}(\xi+2, \xi, \sigma) + S^{(1)}(\zeta, \xi, \sigma)\,\mathrm{d}\zeta. \qquad (4.24)$$

Equations (4.17) and (4.24) are a system of equations determining $F(\xi, \sigma)$ and $S^{(1)}(\psi_0, \sigma)$, since $r^{(0)}$ can be expressed in terms of F and $S^{(1)}$ via (4.5) (replacing $T^{(1)}$ by $\omega T^{(1)}$), an expansion of (2.20b) and the result (3.17b) for $P^{(1)}$.

Owing to the coupling of $S^{(1)}$ and $P^{(1)}$ via the integrals in (4.17) and (4.24), an explicit solution is not available. Thus we have performed numerical integrations, which will now be discussed.

5. Numerical evaluations

5.1. *Finite-difference approximations*

In order to evaluate the system of equations (4.17), (4.24), (3.17b) for $S^{(1)}$ and F, one has to employ a numerical method that yields non-oscillating approximations near discontinuities of F, because effects of numerical oscillations on the calculated time to ignition could hardly be distinguished from those of the desired perturbations. We use an explicit two-step upwind-differencing scheme, proposed by van Leer (1984) and Munz (1985) to approximate solutions to the nonlinear equation for F. The secular equation (4.17) for $S^{(1)}$ is integrated with the Eulerian predictor–corrector method. The integrals are evaluated by means of the trapezoidal rule. The coupling of F and $S^{(1)}$ is taken into account by simultaneous solution of the equations. The
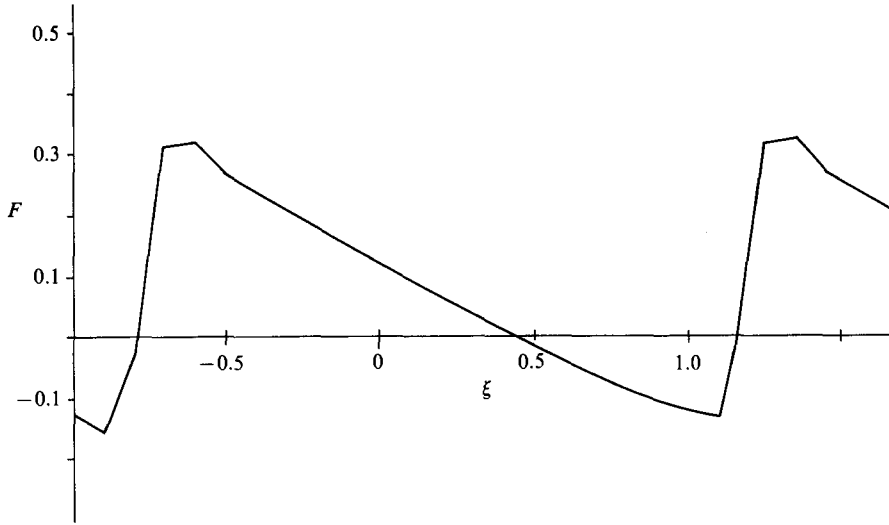
FIGURE 10. Non-oscillating approximation to $F(\xi, \sigma)$ a short time before ignition on a mesh with step size $\Delta\xi = \frac{1}{10}$.

scheme of van Leer and Munz is based on a first-order scheme designed to approximate weak solutions of nonlinear scalar conservation laws of the form

$$F_\sigma + G_\xi = 0, \tag{5.1}$$

where G may be considered as the flux of F in the (ξ, σ)-space, when σ is associated with the time.

The idea is to construct a numerical flux $g(v, w)$ to reproduce the conservation properties of the original equation by setting

$$F_i^{n+1} = F_i^n - \lambda[g(F_i^n, F_{i+1}^n) - g(F_{i-1}^n, F_i^n)], \tag{5.2}$$

where F_i^n is an approximation to $F(i\Delta\xi, n\Delta\sigma)$, $\lambda = \Delta\sigma/\Delta\xi$, and $\Delta\xi, \Delta\sigma$ are the discretization parameters. The numerical flux is designed such that it is consistent with $G(F)$, i.e.

$$g(F, F) = G(F),$$

and that the total variation $TV^n \equiv \Sigma_i|F_{i+1}^n - F_i^n|$ diminishes with increasing σ. This ensures that unphysical oscillations are avoided, and is called the total variation diminishing (TVD) property. Second-order accuracy is obtained at least in regions of smooth $F(\xi, \sigma)$ by introduction of preliminary linear approximations to $F(\xi, \sigma)$ within the interval $[(i - \frac{1}{2})\Delta\xi, (i + \frac{1}{2})\Delta\xi]$ and by performing a predictor step to estimate the fluxes in $\sigma = (n + \frac{1}{2})\Delta\sigma$.

With a suitable choice of the slopes of the preliminary linear structures next to steep gradients this procedure ensures the TVD-property, such that a sharp resolution of discontinuities is obtained corresponding to the second-order accuracy in smooth regions, but without oscillations in the vicinity.

The secular equation (4.24) for F can be transformed to conservation form according to (5.1) when the flux G is defined by

$$G[F(\xi, \sigma); F, \sigma] = \frac{\Gamma}{P_0(\sigma)} \left(\tfrac{1}{2}F^2(\xi, \sigma) + \bar{F}(\sigma) F(\xi, \sigma)\right). \tag{5.4}$$

   Introduction of a source term in the difference scheme is straightforward, although one has to bias the evaluations of the right-hand side with the direction of the characteristics in the (ξ, σ)-space, as proposed by Roe (1986). Figure 10 shows a typical profile of an approximation to $F(\xi, \sigma)$ a short time before ignition. It is seen that oscillations are avoided.

   An additional modification of the difference scheme is necessary in the vicinity of steep gradients, which represent discontinuities in the approximation. The numerical scheme is designed to conserve the quantity F across discontinuities, but here F is related to the pressure p by means of (3.5), (3.17b) and (2.20), and thus it is not conserved. However, the total energy of the system is conserved and a tedious calculation, which accounts for the excess energy formally contained in multivalued regions of the asymptotic solution, allows us to derive the velocity of discontinuities of F in the (ξ, σ)-space as a functional of F and $S^{(1)}$. On the other hand, this velocity can be related to a production of F within the discontinuity. Therefore one can add a source or sink wherever steep gradients in F_i^n occur, such that the correct velocities of discontinuities are obtained. However, numerical experiments have shown that the times to ignition depend only weakly on this effect.

5.2. *Discussion*

In this section we shall discuss the influences of the temperature sensitivity of the reaction rate, the pressure-wave amplitudes, the frequency of the pressure-wave reflections and of the rate of bulk compression. These four aspects are quantified by the non-dimensional activation energy $E = 1/\epsilon$ and by three ratios of characteristic times t'_s/t'_g, t'_I/t'_s and t'_I/t'_p. Let us recall that t'_s/t'_g measures the initial wave amplitude, while t'_I/t'_s is roughly the number of wave reflections that can occur before ignition. Since the reference time t'_a obeys $t'_a = t'_I$ in this section, it follows that $t'_I/t'_s = 1/M$ from (2.16c). The third ratio t'_I/t'_p quantifies the rate of overall compression. While E, t'_I, t'_s and t'_p are already provided by (2.2), (2.4) and (2.6), the definition of t'_g (i.e. of u'_g in (2.5)) used in this section will follow from (5.5).

   In addition to these parameters one may prescribe the initial wave profile and the course of the overall compression by specifying $F(\xi, 0)$ and the piston displacement $v(t)$ defined in (4.2), respectively. The results to be presented below are obtained by taking either N-waves,

$$F(\xi, 0) = \frac{1}{2}\frac{t'_I}{t'_g}[\xi - 2K(\xi)], \qquad (5.5)$$

or sinusoidal waves,

$$F(\xi, 0) = F_{\text{sin}} \sin[\pi(\xi - 2K(\xi))], \qquad (5.6)$$

as initial wave profiles. Equation (5.5) defines t'_g to be the characteristic time of the gas motion based on the maximum speed of a linear initial disturbance (cf. (3.16b) and (2.5)). When the results for different profiles of the initial waves are compared, it is convenient to choose the amplitudes such that the average reaction rates

$$\frac{1}{4}\int_{-1}^{1}\int_{\xi}^{\xi+2} r^{(0)}(\xi, \eta, \sigma)\,d\eta\,d\xi \qquad (5.7)$$

coincide for $\sigma = 0$ and for all profile functions $F(\xi, 0)$ that are compared. This defines t'_g for other than the N-wave profiles of (5.5). Where a mean-field compression is taken into account, we have assumed $\dot{v} = \text{const.} = t'_I/t'_p$ throughout.

   In our calculations we have compared the times to ignition, $t'_{I, p}$ and $t'_{I, v}$ under perturbed and under homogeneous conditions, respectively, and in general observe
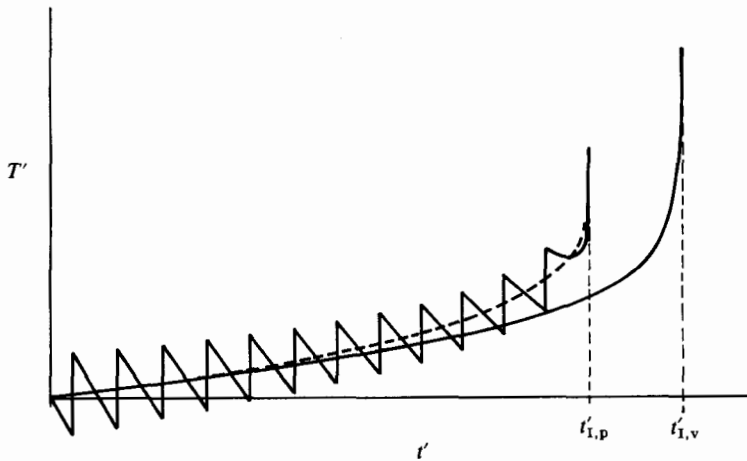
R. Klein and N. Peters

FIGURE 11. The acceleration of the thermal runaway due to gasdynamic perturbations.
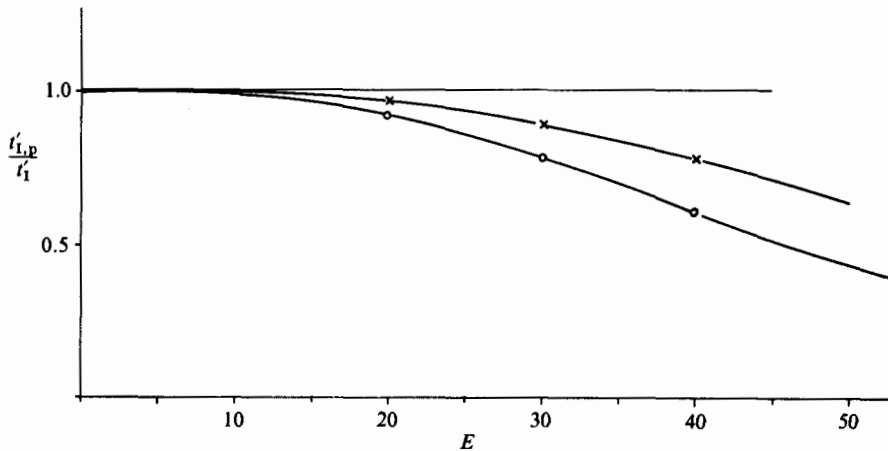

FIGURE 12. Activation energy and relative time to ignition. $U_p \equiv 0, t_s'/t_g' = \frac{1}{8}, t_I'/t_s' = 16$: —×—, initially N-shaped waves; —○—, initially sinusoidal waves.

a shortening of the times to ignition due to the perturbations. This acceleration is a consequence of the nonlinearity of the reaction-rate expression, which is preserved even in the asymptotic expansion (cf. (4.15)). The nonlinearity results in average reaction rates along the curves of integration C_ξ, C_η (cf. (4.23)) that are significantly larger than the reaction rates evaluated with the average temperatures. The overall effect is schematically illustrated in figure 11, where it is seen how in the perturbed flow the average temperature deviates from that of the homogeneous flow, thereby shortening the time to ignition.

In order to isolate the influence of the pressure waves from that of the mean-field compression, we first set $v \equiv 0$ and discuss the ratio $t_{I,p}'/t_I'$. In figure 12 we show the effect of a varying activation energy E with $t_I'/t_s' = 1/M$ and t_s'/t_g' fixed, i.e. for a given gasdynamic situation. The progressive shortening of the time to ignition with increasing E is due to the increase of $\omega = EM$ in the exponential in (4.15) which, for
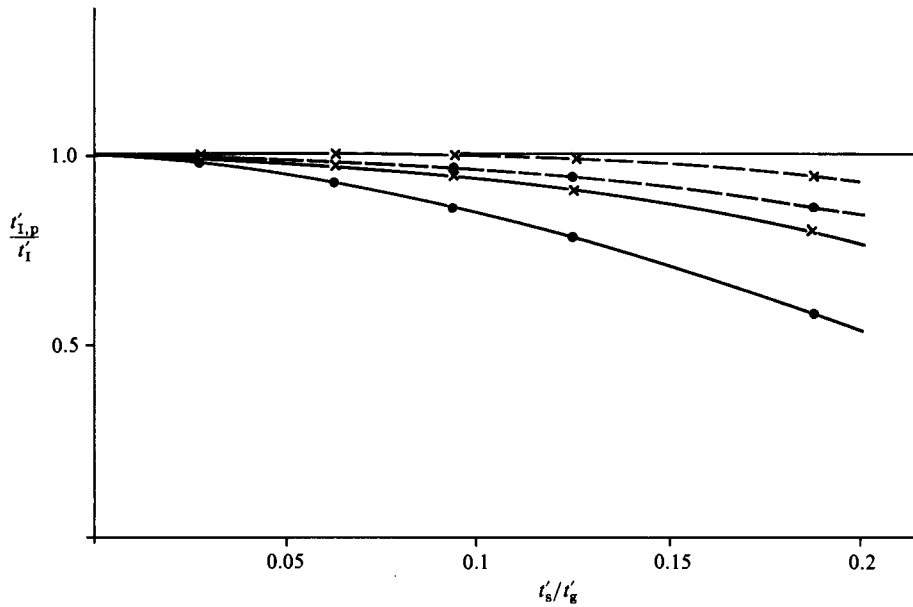
FIGURE 13. Influence of the initial wave amplitude, represented by t'_s/t'_g on the relative time to ignition. $U_p \equiv 0, t'_I/t'_s = 16$: — — — —, $E = 20$; ———, $E = 30$; — × —, initially N-shaped waves; —○—, initially sinusoidal waves.
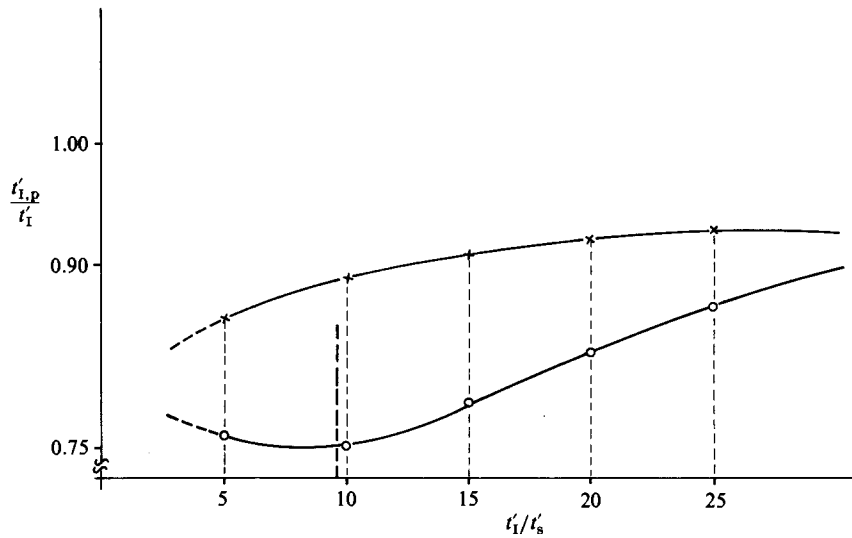

FIGURE 14. The influence of the ignition delay time t'_I on the shortening of the time to ignition $t'_{I,p}$ under a fixed gasdynamic situation. $U_p \equiv 0$, $t'_s/t'_g = \frac{1}{8}$, $E = 30$: — × —, initially N-shaped waves; — ○ —, initially sinusoidal waves.

a given amplitude of the temperature perturbations, strengthens the influence of the nonlinearity.

In order to obtain the results of figure 13 we have fixed E and t'_I/t'_s, and varied the pressure-wave amplitudes, represented by t'_s/t'_g. In addition to the general effect of the perturbations discussed above, a considerable influence of the initial wave profile
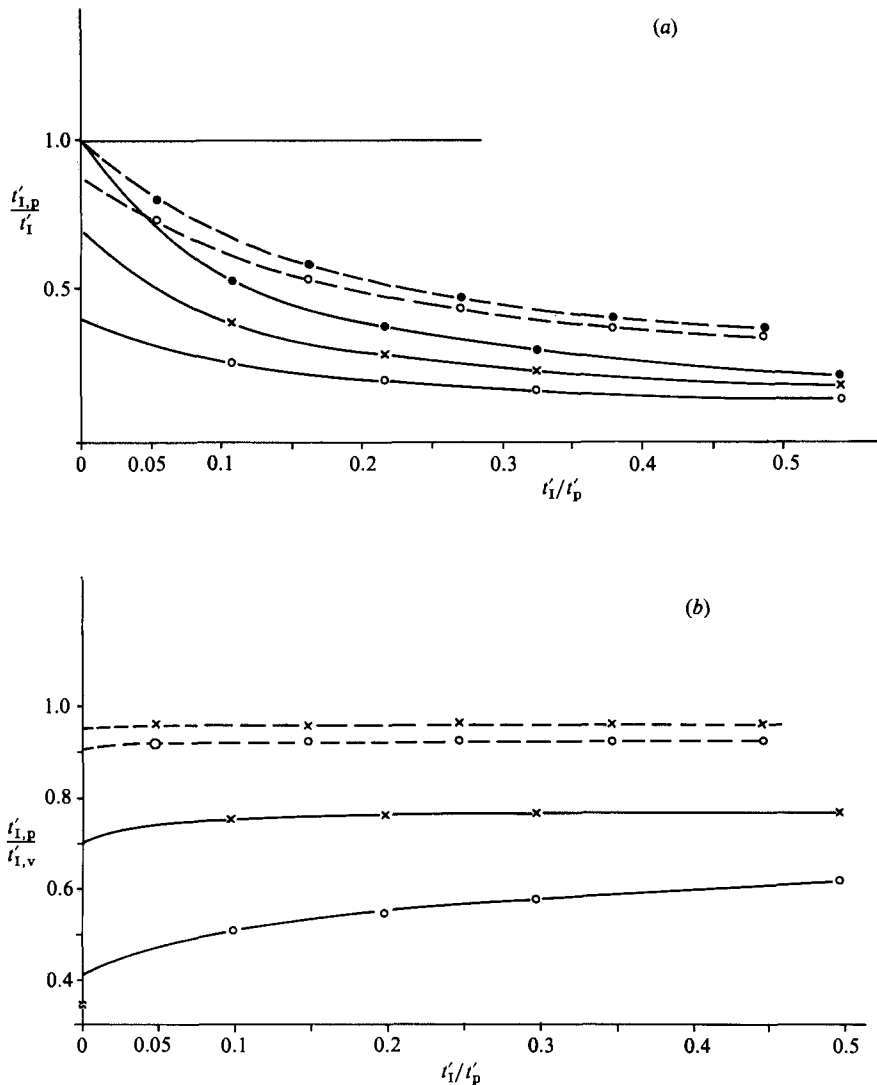
FIGURE 15. (a) Absolute time to ignition measured in units of the dimensional time to ignition under constant density t'_I for varying rates of compression: — ● —, homogeneous compression; — × —, initially N-shaped waves, — ○ —, initially sinusoidal waves; — — — —, $E = 30$, ———, $E = 50$. (b) Comparison of the time to ignition $t'_{I,p}$ under perturbed conditions, and $t'_{I,v}$ under homogeneous conditions, for varying rates of compression.

is observed. The initially smooth sinusoidal waves lead to a stronger acceleration of the process than the N-waves. This effect can be explained with the aid of figure 7, showing the path of a shock wave in the Lagrangian space, and the characteristics that meet the shock from ahead and from behind. In the present first-order approximation the information carried by the characteristics that cross a shock merely determines its local direction but has no more influence in the following evolution. Owing to its nonlinearity the reaction rate is more sensitive to the related cutoff of information at higher temperatures than to that at low-temperature states. The result is a lowering of the average reaction rates compared with a system without discontinuities, in which all information is retained. Thus as long as the sine waves

have not yet formed shocks, they provide larger average reaction rates and hence a stronger acceleration of the process.

The results of a variation of $1/M = t'_I/t'_s$ with fixed E and t'_s/t'_g are shown in figure 14. Keeping $t'_s/t'_g = $ const. we again preserve the gasdynamic situation. The shortening of the time to ignition decreases with a growing number of wave reflections prior to ignition, which is $O(t'_I/t'_s)$. This may be explained by the weakening of the shock waves after multiple reflections, as already discussed in §3. Accordingly, for the sinusoidal waves this effect arises only if there is enough time for the waves to steepen up to weak shocks. This explains the course of the lower curve in figure 14.

The influence of an $O(\epsilon^2)$-mean-field compression is shown in figure 15 (a,b). While figure 15 (a) shows the ratio $t'_{I,p}/t'_I$, measuring the absolute time to ignition $t'_{I,p}$ in units of the ignition delay time t'_I, figure 15 (b) gives the ratio $t'_{I,p}/t'_{I,v}$, comparing the times to ignition under perturbed and unperturbed conditions, but both with an overall compression. The absolute shortening of the time to ignition in figure 15 (a) is of course expected, whereas it is seen in figure 15 (b) that the overall compression has only a weak influence on the excess effect of the pressure waves.

6. Conclusions

A perturbation method combining the analytical method of characteristics with multiple timescaling is developed for the classical piston–cylinder problem, including a slow mean-field compression and acoustic perturbations. The chemically inert case is considered, as well as that of an explosive mixture. The interaction of the explosive chemical reaction with multiple reflected pressure waves or weak shocks is described, in a regime where the amplitude of the gasdynamical disturbances suffices to enhance the reaction rate by an amount of order unity.

To leading order a secular equation is derived which shows the slow mean pressure change due to the accumulation of many reflected waves.

The corresponding first-order equations reveal two important effects: although the principal step in the analysis is a linearization of the gasdynamic equations around a slowly varying mean field, the multiple timescaling allows one to describe slow deformations of the pressure wave profiles. Thus the method is capable of describing weak shock formation, when smooth initial conditions are prescribed.

The second effect concerns the thermal runaway of the chemical reaction. The method is extended to the problem of chemical–acoustic interactions introducing a distinguished limit for small Mach numbers and large activation energies. It is shown how the accumulation of second-order pressure perturbations, caused by thermal expansions of the reacting gas, leads to an additional increase of the first-order pressure. The latter in turn enters into the reaction-rate expression, causing enhanced thermal expansions and thus closing a cycle of interactions. As a result one obtains a considerable shortening of the time to ignition, as compared to the case of a slow homogeneous compression.

This acceleration of the induction process may be important for the problem of engine knock, since it enlarges the probability of self-ignition within the end gas before the arrival of the flame.

Appendix A. Transformation to characteristic form

We define directional time derivatives along a line c in the (ψ, τ)-plane by

$$\left(\frac{\partial}{\partial \tau}\right)_c = \frac{\partial}{\partial \tau} + u_c \frac{\partial}{\partial \psi}, \tag{A 1}$$

$$u_c = \left(\frac{\partial \psi}{\partial \tau}\right)_c. \tag{A 2}$$

Now we search for linear combinations of (2.18), in which only one type of directional derivative appears. This will lead to one set of equations for the slopes u_c of the characteristic lines and a second set of compatibility relations giving constraints for changes of the dependent variables along these lines.

A general linear combination of (2.18), with time coordinate $\tau = t/M$ instead of t, is

$$\left[\lambda_3 - \lambda_1 \frac{p}{T^2}\right]\frac{\partial T}{\partial \tau} + \left[\lambda_1 \frac{1}{T} - \lambda_3 \frac{\gamma-1}{\gamma}\frac{T}{p}\right]\frac{\partial p}{\partial \tau} + [\lambda_2]\frac{\partial p}{\partial \psi}$$

$$+ \gamma[\lambda_2 M]\frac{\partial u}{\partial \tau} + \left[\lambda_1 M \frac{p^2}{T^2}\right]\frac{\partial u}{\partial \psi} + [\lambda_4]\frac{\partial Y}{\partial \tau} = [\lambda_3(-\Delta h) - \lambda_4] M \epsilon r. \tag{A 3}$$

Two equations of the desired type follows from choosing $\lambda_1 = \lambda_2 = 0$, since (2.18c, d) already contain only derivatives along lines $\psi = $ const. Thus these two equations can be retained. We obtain two more equations by requiring the form (A 1):

$$\frac{\lambda_1}{\lambda_2}\frac{1}{T} - \frac{\lambda_3}{\lambda_2}\frac{\gamma-1}{\gamma}\frac{T}{p} = \frac{1}{u_c}, \quad \frac{\lambda_2}{\lambda_1}\gamma\frac{T^2}{p^2} = \frac{1}{u_c}. \tag{A 4a,b}$$

Since $\partial T/\partial \psi, \partial Y/\partial \psi$ do not appear in (A 3) the coefficients of $\partial T/\partial \tau, \partial Y/\partial \tau$ have to vanish,

$$\frac{\lambda_3}{\lambda_1} = \frac{p}{T^2}, \quad \lambda_4 = 0. \tag{A 5a,b}$$

From (A 4) and (A 5a) we have

$$\frac{1}{u_c} = \frac{\lambda_1}{\lambda_2}\left(\frac{1}{T} - \frac{\gamma-1}{\gamma}\frac{1}{T}\right) = \frac{\lambda_1}{\lambda_2}\frac{1}{\gamma}\frac{1}{T} = \frac{\lambda_2}{\lambda_1}\frac{T^2}{p^2}\gamma, \tag{A 6}$$

or

$$\frac{\lambda_1}{\lambda_2} = \pm\gamma\frac{T^{\frac{3}{2}}}{p},$$

and again from (A 4)

$$u_c = \pm\frac{p}{T^{\frac{1}{2}}} = \pm\rho T^{\frac{1}{2}}. \tag{A 7}$$

This is the velocity of acoustic disturbances in the Lagrangian space.

The choice

$$\lambda_1 = \gamma T, \quad \lambda_4 = 0 \tag{A 8}$$

results in

$$\lambda_2 = \frac{p}{T^{\frac{1}{2}}}, \quad \lambda_3 = \frac{\gamma p}{T}, \tag{A 9}$$

and by means of (A 3)

$$\frac{\partial p}{\partial \tau} \pm \frac{p}{T^{\frac{1}{2}}}\frac{\partial p}{\partial \psi} \pm \gamma M \frac{p}{T^{\frac{1}{2}}}\left[\frac{\partial u}{\partial \tau} \pm \frac{p}{T^{\frac{1}{2}}}\frac{\partial p}{\partial \psi}\right] = \epsilon M \gamma \frac{p}{T}(-\Delta h) r. \tag{A 10}$$

With the definition (A 1) we may write

$$\left.\frac{\partial p}{\partial \tau}\right|_{\pm} \pm M\gamma \frac{p}{T^{\frac{1}{2}}} \left.\frac{\partial u}{\partial \tau}\right|_{\pm} = \epsilon M\gamma \frac{p}{T}(-\Delta h)\,r. \tag{A 11}$$

Replacing T by $S^2 P^2$ according to (2.20b), the final result is

$$\left.\begin{aligned}
\frac{\partial P}{\partial \xi} + M\frac{\gamma-1}{2}\frac{1}{S}\frac{\partial u}{\partial \xi} &= \epsilon M\frac{\gamma-1}{2}\frac{(-\Delta h)\,r}{PS^2}\frac{\partial \tau}{\partial \xi}, \\
\frac{\partial P}{\partial \eta} - M\frac{\gamma-1}{2}\frac{1}{S}\frac{\partial u}{\partial \eta} &= \epsilon M\frac{\gamma-1}{2}\frac{(-\Delta h)\,r}{PS^2}\frac{\partial \tau}{\partial \eta}.
\end{aligned}\right\} \tag{A 12}$$

Here we have introduced ξ, η as new coordinates on the set of characteristic lines. Equation (A 7) prescribes the directions of lines of constant ξ and η; thus we have

$$\left.\begin{aligned}
\frac{\partial \psi}{\partial \xi} - \frac{P^\Gamma}{S}\frac{\partial \tau}{\partial \xi} &= 0, \\
\frac{\partial \psi}{\partial \eta} + \frac{P^\Gamma}{S}\frac{\partial \tau}{\partial \eta} &= 0,
\end{aligned}\right\} \tag{A 13}$$

where

$$\frac{p}{T^{\frac{1}{2}}} = \frac{P^\Gamma}{S}; \quad \Gamma = \frac{\gamma+1}{\gamma-1}.$$

Appendix B. Compatibility along wave path to second order, and secular equations to first order

With respect to the leading- and first order-solutions (3.5), (3.7) and (3.16), we rewrite the right-hand side of (3.10b) as

$$\left.\begin{aligned}
-\tfrac{1}{2}(P^{(1)}_\sigma + u^{(0)}_\sigma) &= +\tfrac{1}{2}\psi_0\,\ddot{P}_0(\sigma) - F_\sigma(\eta, \sigma), \\
-\tfrac{1}{2}(P^{(1)}_\sigma - u^{(0)}_\sigma) &= -\tfrac{1}{2}\psi_0\,\ddot{P}_0(\sigma) - F_\sigma(\xi, \sigma).
\end{aligned}\right\} \tag{B 1}$$

Then integration of (3.10b) along $\eta = $ const. and $\xi = $ const. yields the general solutions

$$\left.\begin{aligned}
P^{(2)} + u^{(1)} &= \tfrac{1}{2}\ddot{P}_0\,\psi_0^2 - 2\psi_0\,F_\sigma(\eta, \sigma) + 2G^{(2)}(\eta, \sigma), \\
P^{(2)} - u^{(1)} &= -\tfrac{1}{2}\ddot{P}_0(1 - \psi_0^2) - 2(1 - \psi_0)\,F_\sigma(\xi, \sigma) + 2F^{(2)}(\xi, \sigma),
\end{aligned}\right\} \tag{B 2}$$

respectively.

With the aid of (B 2) we can eliminate either $P^{(2)}$ or $u^{(1)}$ to obtain (3.35). Evaluation of (3.35) at the boundaries and use of the conditions (3.13b) and (3.14b) first gives

$$G^{(2)}(\eta, \sigma) = F^{(2)}(\eta, \sigma) - \tfrac{1}{4}\ddot{P}_0 - F_\sigma(\eta, \sigma) + u^{(1)}_c, \tag{B 3}$$

and then leads to a recursion formula for $F^{(2)}$:

$$F^{(2)}(\xi - 2, \sigma) - F^{(2)}(\xi, \sigma) = (u^{(1)}_p - u^{(1)}_c) + 2F_\sigma(\xi, \sigma). \tag{B 4}$$

A corresponding recursion for $P^{(2)}$ follows when the periodicity of all leading- and first-order functions with respect to a translation $(\xi, \eta) \rightarrow (\xi + 2, \eta + 2)$ is taken into account.

For (B 3) this means

$$G^{(2)}(\eta+2,\sigma)-G^{(2)}(\eta,\sigma) = F^{(2)}(\eta+2,\sigma)-F^{(2)}(\eta,\sigma), \tag{B 5}$$

and for (3.35 b)

$$P^{(2)}(\xi+2,\eta+2,\sigma)-P^{(2)}(\xi,\eta,\sigma)$$
$$= [F^{(2)}(\xi+2,\sigma)-F^{(2)}(\xi,\sigma)]+[F^{(2)}(\eta+2,\sigma)-F^{(2)}(\eta,\sigma)]. \tag{B 6}$$

Since the brackets on the right-hand side of this equation also show the periodicity, as can be seen with the aid of (3.16), (3.18), (3.21), (3.34) and (B 4), an n-fold application of (B 6) results in

$$P^{(2)}(\xi+2n,\eta+2n,\sigma)-P^{(2)}(\xi,\eta,\sigma)$$
$$= n[(F^{(2)}(\xi+2,\sigma)-F^{(2)}(\xi,\sigma)]+[F^{(2)}(\eta+2,\sigma)-F^{(2)}(\eta,\sigma)]. \tag{B 7}$$

The same arguments that led to the secular equation (3.21) for $P^{(0)}$ now require

$$F^{(2)}(\xi+2,\sigma)-F^{(2)}(\xi,\sigma) \equiv 0, \tag{B 8}$$

and with (B 4), (3.16 a) and (3.17) this is the result already given in (3.38).

Appendix C.

We want to replace the operator $(\partial/\partial\tau)|_\psi$ by an expansion that only uses derivatives with respect to the set of coordinates ψ_0, ϕ, σ according to (4.11) and (4.12). The Lagrangian coordinates ψ, τ are expanded as

$$\tau = \frac{1}{M}t_0(\sigma)+\delta\tau^{(1)}+\delta^2\tau^{(2)}+\dots, \tag{C 1a}$$

$$\psi = \psi_0+\delta\psi^{(1)}+\delta^2\psi^{(2)}+\dots, \tag{C 1b}$$

and $\psi^{(i)}$ and $\tau^{(i)}$ are here considered to be functions of (ψ_0,ϕ,σ). Thus we have a transformation

$$(\psi,\tau,\delta) \leftrightarrow (\psi_0,\phi,\sigma). \tag{C 2}$$

In the following we denote partial derivatives with respect to (ψ,τ,δ) by

$$\frac{\partial}{\partial\psi}, \quad \frac{\partial}{\partial\tau}, \quad \frac{\partial}{\partial\delta},$$

and those with respect to (ψ_0,τ,σ) by

$$\partial_{\psi_0}, \quad \partial_\phi, \quad \partial_\sigma, \tag{C 3}$$

or by subscripts on the function F:

$$F_{\psi_0}, \quad F_\phi, \quad F_\sigma. \tag{C 4}$$

Generally we have

$$\frac{\partial}{\partial\tau} = \frac{\partial\phi}{\partial\tau}\partial_\phi+\frac{\partial\psi_0}{\partial\tau}\partial_{\psi_0}+\frac{\partial\sigma}{\partial\tau}\partial_\sigma. \tag{C 5}$$

Since, according to (3.4) and (4.11),

$$\sigma(\psi,\tau,\delta) = \delta\phi(\psi,\tau,\delta), \tag{C 6}$$

(C 5) reads

$$\frac{\partial}{\partial \tau} = \frac{\partial \phi}{\partial \tau}(\partial_\phi + \delta \partial_\sigma) + \frac{\partial \psi_0}{\partial \tau} \partial_{\psi_0}. \qquad (C\ 7)$$

Now $\partial \psi_0 / \partial \tau$ and $\partial \phi / \partial \tau$ are to be examined. We have

$$\psi = \psi_0 + \delta \psi^{(1)} + \delta^2 \psi^{(2)} + \dots . \qquad (C\ 8)$$

Thus

$$\frac{\partial \psi_0}{\partial \tau} = -\delta \frac{\partial \psi^{(1)}}{\partial \tau} - \delta^2 \frac{\partial \psi^{(2)}}{\partial \tau} - \dots .$$

By means of the expansion (C 1 a) and the relation (C 7) we can express $\partial \tau / \partial \tau \equiv 1$ in the form

$$1 = \frac{\delta}{M} \frac{\mathrm{d}t_0}{\mathrm{d}\sigma} \frac{\partial \phi}{\partial \tau} + \delta \left(\tau_{\psi_0}^{(1)} \frac{\partial \psi_0}{\partial \tau} + \tau_\phi^{(1)} \frac{\partial \phi}{\partial \tau} \right) + \delta^2 \left(\tau_\sigma^{(1)} \frac{\partial \phi}{\partial \tau} + \tau_\phi^{(2)} \frac{\partial \phi}{\partial \tau} + \tau_{\psi_0}^{(2)} \frac{\partial \psi_0}{\partial \tau} \right) + \dots . \qquad (C\ 9)$$

Using (3.9) to obtain $(\delta/M)\,\mathrm{d}t_0/\mathrm{d}\sigma = P_0^{-\Gamma}$, and replacing $\partial \psi_0 / \partial \tau$ by (C 8), one obtains a second-order approximation for $\partial \phi / \partial \tau$:

$$\frac{\partial \phi}{\partial \tau} = P_0^\Gamma \{1 - \delta P_0^\Gamma \tau_\phi^{(1)} + \delta^2 [\tfrac{1}{2} P_0^{2\Gamma}(\tau_\phi^{(1)})^2 - P_0^\Gamma(\tau_\sigma^{(1)} + \tau_\phi^{(2)} - \tau_{\psi_0}^{(1)} \psi_\phi^{(1)})]\} + O(\delta)^3. \qquad (C\ 10)$$

Now one may use (C 7) and (C 10) in (C 8) to eliminate the τ-derivatives by iteration:

$$\frac{\partial \psi_0}{\partial \tau} = -\delta \psi_\phi^{(1)} P_0^\Gamma + \delta^2 P_0^\Gamma [P_0^\Gamma \tau_\phi^{(1)} \psi_\phi^{(1)} + \psi_{\psi_0}^{(1)} \psi_\phi^{(1)} - (\psi_\phi^{(2)} + \psi_\sigma^{(1)})] + O(\delta^3). \qquad (C\ 11)$$

Equation (C 7) together with (C 10) and (C 11) enables us to express $\partial/\partial \tau|_\psi$ in terms of partial derivatives with respect to (ψ_0, ϕ, σ) with second-order accuracy, if the coordinate functions $\psi^{(1)}, \psi^{(2)}, \tau^{(1)}, \tau^{(2)}$ are given in terms of (ψ_0, ϕ, σ) or (ξ, η, σ). The final result is

$$\frac{\partial}{\partial \tau} = P_0^\Gamma \{\partial_\phi + \delta(\partial_\sigma - P_0^\Gamma \tau_\phi^{(1)} \partial_\phi - \psi_\phi^{(1)} \partial_{\psi_0})$$
$$+ \delta^2 [\tfrac{1}{2} P_0^{2\Gamma}(\tau_\phi^{(1)})^2 - P_0^\Gamma(\tau_\phi^{(2)} + \tau_\sigma^{(1)} - \tau_{\psi_0}^{(1)} \psi_\phi^{(1)})] \partial_\phi - \delta^2 P_0^{2\Gamma} \tau_\phi^{(1)} \partial_\sigma$$
$$+ \delta^2 [P_0^\Gamma \tau_\phi^{(1)} \psi_\phi^{(1)} + \psi_\phi^{(1)} \psi_{\psi_0}^{(1)} - (\psi_\phi^{(2)} + \psi_\sigma^{(1)})] \partial_{\psi_0} + O(\delta^3)\}. \qquad (C\ 12)$$

$S^{(0)}$ and $Y^{(0)}$ are set to unity and hence there is no need to calculate $\psi^{(2)}, \tau^{(2)}$ when we carry out the second-order expansions of the (2.26 c, d) for S and Y in order to obtain secular conditions for $S^{(1)}$ and $Y^{(1)}$.

REFERENCES

CLARKE, J. F. 1978 Small amplitude gasdynamic disturbances in an exploding atmosphere. *J. Fluid Mech.* **89**, 343–355.

CLARKE, J. F. & CANT, R. S. 1984 Nonsteady gasdynamic effects in the induction domain behind a strong shock wave. In *Dynamics of Explosions and Reactive Systems. Progress in Astronautics and Aeronautics*, vol. 95 (ed. J. R. Bowen), pp. 142–163. Springer.

KLUWICK, A. 1981 The analytical method of characteristics. *Rev. Prog. Aerospace Sci.* **19**, 197–313.

MUNZ, C. D. 1985 Näherungs verfahren höherer Ordnung zur Approximation von Stoßwellen. *Bericht Nr.* 28, Mathemat. Inst. II Univ., Karlsruhe.

ROE, P. L. 1986 Upwind differencing schemes for hyperbolic conservation laws with source terms. In *Nonlinear Hyperbolic Problems* (ed. A. Dold & B. Eckmann). Lecture Notes in Mathematics, vol. 1270, pp. 41–50. Springer.

RHADWAN, R. H. & KASSOY D. R. 1984 The response of a confined gas to a thermal disturbance: rapid boundary heating. *J. Engng Maths*, **18**, 133–156.

SCHNEIDER, G. H. 1979 Kompression und Expansion eines Gases in einem Zylinder als Störproblem. Dissertation, Wien.

SCHNEIDER, W. 1978 *Mathematische Methoden der Strömungsmechanik*. Vieweg.

SEIFERT, H. 1962 *Instationäre Strömungsvorgänge in Rohrleitungen an Verbrennungskraftmaschinen*. Springer.

VAN LEER, B. 1984 On the relation between the upwind differencing schemes of Godunov, Enquist-Osher, and Roe. *SIAM J. Sci. Stat. Comp.* **5**, 1–21.

WHITHAM, G. B. 1974 *Linear and Nonlinear waves*. Wiley.